Distribution Agreement

In presenting this thesis as a partial fulfillment of the requirements for a degree from Emory University, I hereby grant to Emory University and its agents the non-exclusive license to archive, make accessible, and display my thesis in whole or in part in all forms of media, now or hereafter now, including display on the World Wide Web. I understand that I may select some access restrictions as part of the online submission of this thesis. I retain all ownership rights to the copyright of the thesis. I also retain the right to use in future works (such as articles or books) all or part of this thesis.

Michelle Lin April 14, 2020

Pentagalloyl glucose: An ethnobotanical approach to multidrug resistance

by

Michelle Lin

Dr. Cassandra Quave
Adviser

Department of Biology

Dr. Cassandra Quave

Adviser

Dr. Victor Corces

Committee Member

Dr. Kate O'Toole

Committee Member

2020

Pentagalloyl glucose: An ethnobotanical approach to multidrug resistance

By

Michelle Lin

Dr. Cassandra Quave

Adviser

An abstract of
a thesis submitted to the Faculty of Emory College of Arts and Sciences
of Emory University in partial fulfillment
of the requirements of the degree of
Bachelor of Science with Honors

Department of Biology

2020

Abstract

Pentagalloyl glucose: An ethnobotanical approach to multidrug resistance

By Michelle Lin

Multidrug resistant *Acinetobacter baumannii* strains pose a significant public health threat in the twenty-first century due to their resistance to multiple antibiotic categories. Effective treatments for nosocomial infections of *A. baumannii* have dwindled as the evolution of resistance has outpaced the development of novel antimicrobials. Here, I applied an ethnobotanical approach to anti-infective drug discovery for *A. baumannii*, by (1) investigating the inhibitory activity of pentagalloyl glucose (PGG) isolated from *Schinus terebinthifolia* (Brazilian peppertree), (2) exploring possible inhibition mechanisms of PGG, and (3) confirming the antimicrobial effects of *Rhus coriaria* (Sicilian sumac) and *Rhus copallinum* (winged sumac), both of which are in the same family (Anacardiaceae) as *S. terebinthifolia*.

Growth inhibition and time-kill assays revealed PGG to be a bacteriostatic agent against *A. baumannii* strains of varying resistance profiles (MIC 64 to 256 μg/mL), as well as *Pseudomonas aeruginosa* (MIC 16 μg/mL) and *Staphylococcus aureus* (MIC 64 μg/mL). Cytotoxicity assays with human keratinocytes revealed an IC_{50} of 256 μg/mL and a therapeutic index of 32, suggesting therapeutic use as topical agent. A 21-day resistance passaging assay of PGG did not produce resistant phenotypes. Iron chelation and lipopolysaccharide attachment were identified as PGG's possible mechanism(s) of action. Finally, *R. coriaria* and *R. copallinum* extracts inhibited growth of *A. baumannii* (MICs of 128 μg/mL), *P. aeruginosa* (MICs of 32 and 64 μg/mL, respectively), *S. aureus* (MICs of 64 and 256 μg/mL, respectively). PGG was determined to be a putative active compound in the *Rhus* extracts. In summation, traditional medicinal plants, like *S. terebinthifolia* and the *Rhus* extracts, provide unexplored avenues of research for the fight against multidrug resistance.

Pentagalloyl glucose: An ethnobotanical approach to multidrug resistance

By

Michelle Lin

Dr. Cassandra Quave

Adviser

A thesis submitted to the Faculty of Emory College of Arts and Sciences
of Emory University in partial fulfillment
of the requirements of the degree of
Bachelor of Science with Honors

Department of Biology

2020

Acknowledgements

To Dr. Quave - Thank you for your guidance throughout the past few years. It has been an incredible honor to be part of the Quave Lab Group - to learn from and work with some of the brightest minds I have met in an environment that is encouraging and supportive. Thank you for giving me the opportunity to learn and grow and for serving as a role model. This project would not have been possible without your support.

To my committee members - Thank you, Dr. Corces and Dr. O'Toole for your encouragement and support. I am honored to have been both a student in your classes, and an Honors Candidate under your instruction. I am incredibly grateful for the many office hours full of questions and discussions about science and the future. Thank you for imparting so much knowledge - both academic and experiential - during my time at Emory University.

To Dr. Lyles - Thank you for your help in the phytochemistry lab and in meetings. Your encouragement to always think critically has helped me in all of my scientific endeavors. I appreciate all of the time and support you have given me.

To Micah Dettweiler - It would be an understatement to simply say that I have learned a great deal from you. Thank you for not only guiding me throughout this project, but also for teaching me during the past couple of years.

To my friends and colleagues in the Quave Lab Group - I know I will dearly miss the Quave Lab Group. I appreciate the kindness and support of this community and am very grateful to have such hardworking and wonderful scientists to look up to.

To my parents - Thank you for encouraging and believing in me, even when I was unsure of myself. Our random phone calls and messages have meant the world to me. I am forever grateful for the love that you show me.

To my friends - Thank you for being there for me every step of the way. Thank you for encouraging me and listening to me.

Funding for this project was provided by our lab's R21 grant, which supports *Acinetobacter baumannii* research in relation to medical ethnobotany.

Table of Contents

List of Tables and Figures

CHAPTER 1: INTRODUCTION

Emergence and spread of highly resistant bacteria

Bacterial resistance to conventional antibiotics used in healthcare, agriculture, and food service poses a challenging international health problem. In healthcare, this public health crisis raises mortality rates, length of hospitalization, and hospital costs for patients infected with antibiotic resistant pathogens (Cosgrove, 2006). A 2006 study performed by clinical researchers at The Johns Hopkins Medical Institution documented a $6,000 to $30,000 increase in hospital costs for patients infected with antibacterial strains, compared to patients infected with susceptible strains (Cosgrove, 2006). The costs of treatment for resistant infections create additional challenges for affected patients and their families. In many instances, patients acquire these resistant infections while being treated for other illnesses in hospitals, and the costs of treating these nosocomial infections, or hospital-acquired infections, extend their hospital bills tremendously. Emerging resistant strains related to nosocomial infections include carbapenem-resistant Enterobacteriaceae, multidrug resistant *Pseudomonas aeruginosa*, and methicillin-resistant *Staphylococcus aureus* (CDC, 2019).

The war on resistant bacteria plays out in the fields of agriculture and food service as well. Individuals who work directly with animals, such as animal care workers like veterinarians, and producers like farmers, are particularly susceptible to any bacterial infections that may plague the animals. In turn, infected individuals may then expose their families, colleagues, and greater community to otherwise isolated antibiotic resistant bacteria (Marshall & Levy, 2011). In addition, current agricultural practices involving the use of antibiotic growth promoters (AGPs) have been associated with increased risk of resistance transference between species (Wegener, Aarestrup, Jensen, Hammerum, & Bager, 1999). These antibiotics are fed to farm animals - not to treat

existing conditions, but rather to promote the production of livestock (Glenn et al., 2013). Because resistance selection can occur under any conditions of increased antimicrobial use, the impact of AGP utilization is being widely investigated. For example, a 2013 study on *Salmonella enterica*, a common food-borne bacterium, described livestock as reservoirs and retail meats as vectors of resistance genes (Glenn et al., 2013). Glenn et al. documented the presence of common resistance genes - such as those conferring resistance to beta-lactams and tetracycline - in the *Salmonella enterica* of animal, retail meat, and human isolates. Another study on livestock infected with methicillin-resistant *S. aureus* (MRSA) showed that contamination can extend from sick farm animals to meat products to human consumers (Price et al., 2012). Thus, food related transmission adds another aspect of risk associated with antibiotic overuse and misuse.

Multidrug resistance (MDR) is defined by the European Centre for Disease Prevention and Control (ECDC) and the Centers of Disease Control and Prevention (CDC) as resistance in at least three antimicrobial categories based on organism or organism group (Magiorakos et al., 2012). MDR bacteria pose a significant threat to infection treatment, particularly in nosocomial infections, because these pathogens have acquired non-susceptibility to most conventional antibiotic treatments (Nikaido, 2009). Patients with compromised immune systems may be impacted even more negatively by these hospital-acquired infections.

In addition to nosocomial MDR bacteria, community associated MDR play a significant role in spreading diseases through shared contact. One typical aspect of community-associated MDR is their stable antibiotic resistance phenotype - this stability is maintained even when there is not selective pressure for resistance (van Duin & Paterson, 2016). Such stability makes community associated MDR another threat to consider when considering the impact and treatment of resistant bacteria.

Acinetobacter baumannii

This Honors Thesis focuses on *Acinetobacter baumannii*, a Gram-negative aerobe with many multidrug resistant strains. *A. baumannii* is an oxidase negative, catalase positive, and nonmotile bacillus that thrives at 20 to 30°C in complex media (Bergogne-Berezin & Towner, 1996). In the environment, this species has been found in water and soil samples, and isolation from aquatic sources and soil samples is possible through an enrichment culture consisting of a low pH medium with carbon and nitrogen supply (Baumann, 1968) . In relation to human microbiology, *A. baumannii* is known to be a common inhabitant of the skin and respiratory tract (Sebeny, Riddle, & Petersen, 2008). However, the common sites of infection indicate an even wider range of hospitable environments for this opportunistic pathogen: skin, respiratory tract, peritoneum, urinary tract (Bergogne-Berezin & Towner, 1996). Other infections associated with *A. baumannii* include bacteremia, which is a condition in which viable bacteria infiltrates the bloodstream, and meningitis, which causes inflammation of the brain and spinal cord meninges (Bergogne-Berezin & Towner, 1996).

Infections with this species are repeatedly noted in certain patient populations: elderly and newborns. In addition, vulnerability to the bacterium increases for patients with burn wounds, immunosuppressed systems, and chronic lung disease, as well as for patients using respiratory and/or gastric equipment and antibiotic therapy (Bergogne-Berezin & Towner, 1996). Examples of medical equipment that may unintentionally serve as breeding grounds for the bacterium include endotracheal tubes and intravenous catheters (Tripathi, Gajbhiye, & Agrawal, 2014).

Virulence factors enhance the bacterium's ability to infect and promote illness in the host on a cellular level. Although the virulence factors of this species are not fully understood yet,

a few factors have been identified in recent years. As summarized in a 2017 review, identified virulence factors include activities of porins, capsular polysaccharide, lipopolysaccharide, phospholipase, outer membrane vesicle, iron acquisition system, zinc acquisition system, manganese acquisition system, Type II protein secretion system, Type VI protein secretion system, Type V protein secretion system, penicillin-binding protein 7/8, and beta-lactamase (Lee et al., 2017). For example, the capsular polysaccharide surrounds the cell wall and provides both physical and microbiological protection from foreign entities (Singh, Adams, & Brown, 2018). On a physical level, the capsular polysaccharide is comprised of repeating sugar units that barricade against host immune cells. On a microbiological level, the layer is associated with increased resistance to antibiotics.

Throughout the 20th century, medical professionals treated infections caused by *A. baumannii* with antibiotics that target key pathways, such as carbapenems that interfere with bacterial cell wall synthesis. However, many strains have developed resistance to common antibiotics in recent decades. The species is considered to be a dangerous opportunistic pathogen in both hospital and community-acquired infections due to its high incidence of resistance to first-line agents (Howard, O'Donoghue, Feeney, & Sleator, 2012). Carbapenem-resistant *A. baumannii,* for example, is acknowledged by the CDC as an "urgent" threat, the highest-level threat assignment given by the CDC. According to the CDC's 2019 Antimicrobial Resistance Report, carbapenem-resistant *A. baumannii* were associated with approximately 8,500 hospitalizations and 700 deaths in the United States in 2017 (CDC, 2019).

Natural products as an alternative to conventional antibiotics

The need for solutions against antibiotic resistance is evident, and discussions surrounding solutions range from global public health interventions to community-based antibiotic stewardship to further drug development. Antibiotic stewardship, in particular, calls for the restriction of antibiotic prescriptions by health care providers. This strategy serves to decrease overuse and misuse of drugs in the treatment of non-relevant illnesses like the flu, so as to discourage the development of further resistance (Laxminarayan et al., 2013). In the research and development fields, antibiotic discovery has slowed tremendously since the 1970s, with fewer antibiotics being developed and fewer classes being explored. Novel antibiotic classes against Gram-negative bacteria, like the aforementioned *A. baumannii*, have not surfaced in recent years while the resistance profiles of the bacteria continue to grow (Laxminarayan et al., 2013). Overall, antibiotic development in the United States is a lengthy process that requires years of dedicated laboratory and clinical research, followed by review and monitoring by the Food and Drug Administration (CDC, 2019). In the modern economy, this has translated to decreased pharmaceutical investment in antibiotic sectors (WHO, 2019). In addition to the general economic challenges that slow traditional antibiotic research, particular biological characteristics of Gram-negative bacteria pose significant difficulties for researchers. Gram-negative bacteria have an outer membrane with a lipopolysaccharide component that inhibit the entry of antibiotics, and the drugs that can successfully gain entry through bacterial porins may be swiftly ejected by efflux pumps (Richter et al., 2017) .

Due to the dwindling array of potent antibiotics and constant emergence of more MDR bacteria from previously susceptible strains, alternative treatment options must be pursued to combat infectious pathogens (Edwards-Jones, 2013). One quickly expanding field of research is the promising field of medical ethnobotany, which applies modern phytochemistry and

microbiology research techniques to traditional medicinal plants for anti-infective drug discovery (Quave & Pieroni, 2015). For millennia, humans have employed the use of plants as natural remedies for illnesses ranging from digestive to skin diseases. Various cultures throughout time, from the Chippewa Native Americans to the Arabic to the New England settlers, have documented ways of identifying, preparing, and applying plant parts. In medical ethnobotany, such documentation has provided valuable sources for the discovery and characterization of novel chemical compounds for drug development.

Previous studies performed by members of our research team (Quave Research Group) have validated the significant contributions that ethnobotanical knowledge may provide for the fight against infectious pathogens. For instance, research of plants utilized by American Civil War physicians showed potential uses of *Quercus alba* for the in vitro growth inhibition of multidrug resistant *S. aureus, Klebsiella pneumoniae,* and *A. baumannii*, among other species (Dettweiler et al., 2019). Another recent study published by the Quave Group identified an active compound in *Gingko biloba* for its antibacterial effects against *Cutibacterium acnes*, *S. aureus*, and *Streptococcus pyogenes* (Chassagne, Huang, Lyles, & Quave, 2019). These discoveries, among the plethora of ethnobotanical discoveries, demonstrate the potential of medicinal plants as sources of anti-infective drugs.

Project aims and research questions

The plants *Rhus coriaria* and *Rhus copallinum,* both in family Anacardiaceae, have traditional medicinal uses and might reveal novel chemicals for drug development. Our lab performs bio-guided fractionation on active extracts in our plant library by performing bio-activity assays on active fractions and then separating the most active fractions; this process eventually

results in the isolation of pure compounds. The Quave Research Group has recently isolated, via bio-guided fractionation focusing on growth inhibition, the active compound pentagalloyl glucose (PGG) from another ethnobotanical plant in the family Anacardiaceae, *Schinus terebinthifolia.* In this Honors Thesis, I apply modern phytochemical and microbiological techniques, such as growth inhibition assays and supplementation assays, to study PGG as a potential treatment against MDR bacteria, particularly against resistant *A. baumannii*.

CHAPTER 2: LITERATURE REVIEW

Past and present: traditional uses and current studies of selected *Rhus* species

The plants *Rhus coriaria* L. and *Rhus copallinum* L., both in family Anacardiaceae, have been used in traditional medicine and cuisine in several cultures throughout history. An analysis of these plants as viable options for bacterial treatment necessitates a review of their historical background and cultural significance. Considerations for how the two *Rhus* species might benefit modern medicine may lie in the scripts of the old, as many ethnobotanists have observed and recorded. Here is an overview of *R. coriaria* and *R. copallinum*, featuring both traditional knowledge and recent scientific studies.

1. *Rhus coriaria* L.

Commonly known as the Sicilian sumac, or elm-leafed sumac, *R. coriaria* is a deciduous plant shrub from southern Europe (Polunin, 1980). At about three meters in height when fully grown, the shrub is often found in rocky areas throughout Mediterranean countries. The plant's fruits are often used in Middle Eastern cuisine, in a spice mixture called Za'atar, which typically consists of crushed sumac, sesame seeds, thyme, oregano, salt, and nutmeg (Facciola, 1990). Likewise, the seed of the plant is used as a condiment of sorts, prepared in similar fashion to mustard (Sturtevant, 1972).

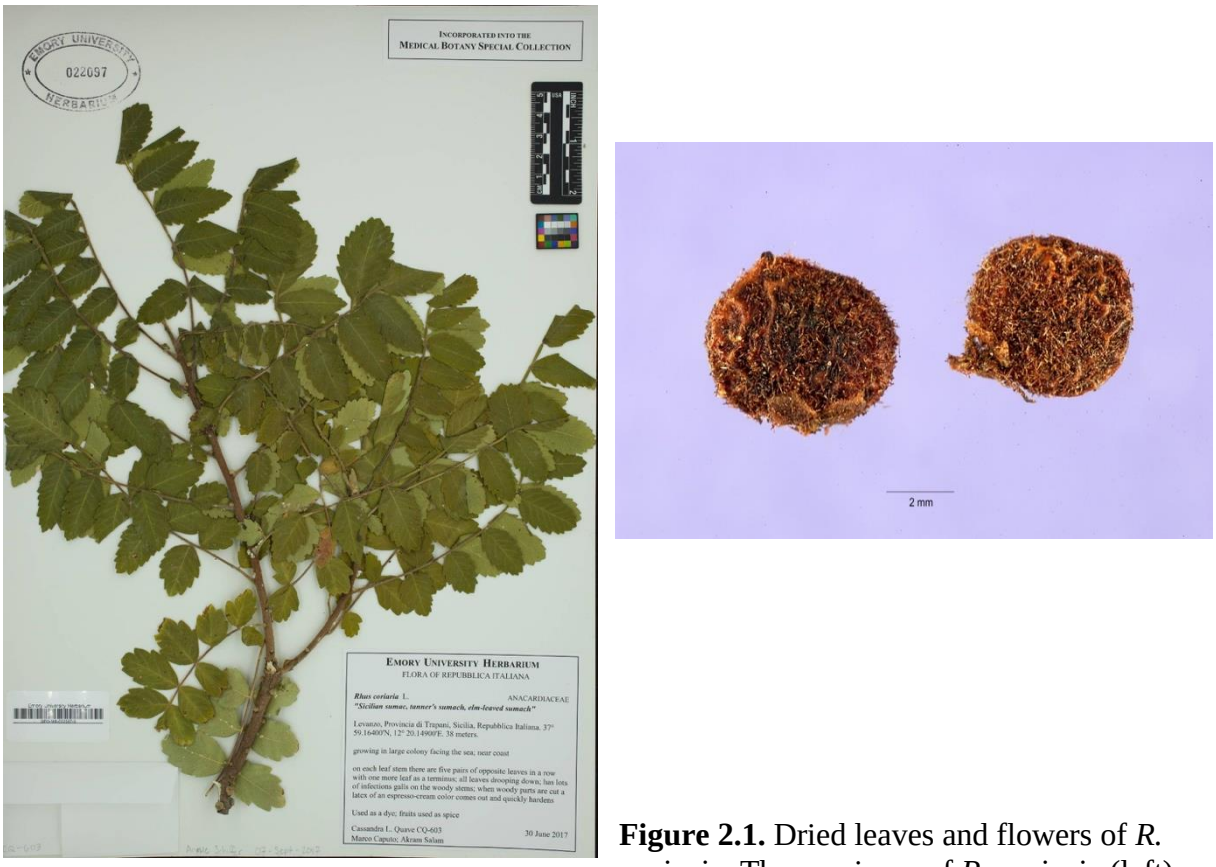

Figure 2.1. Dried leaves and flowers of *R. coriaria.* The specimen of *R. coriaria* (left) was collected from Levanzo, Italy by members of the Emory Herbarium and can be viewed at the Emory University Herbarium. Pictured left are dried leaves, and pictured right are dried flowers from the plant. Source (right): Tracey Slotta, hosted by the USDA-NRCS PLANTS Database (USDA, 2020).

There is known medicinal use of *R. coriaria* as well. For example, in Turkey, the fruit has been used as a treatment for diarrhea; after preparation as a condiment, it is served on boiled eggs (Sezik et al., 2001). Locally known in Turkey as "Tetra agaci sumak", the fruit may also be prepared in a decoction for treatment of ulcers (Tuzlaci & Aymaz, 2001). In Arabic countries, a decoction is orally ingested for problems related to the liver, digestive tract, and urinary system. In the medieval Jewish community of Cairo, the plant was used for "eye diseases, dentistry, abortifacient, and sore throat" as was cited in the medicinal books of Cairo Genizah, a storage

library from a synagogue dating back to the 11th century (Said, Khalil, Fulder, & Azaizeh, 2002) (Lev, 2007). In ancient Cyprus, texts from a monastery reveal *R. coriaria* was used for internal hemorrhages and the common cold. This information was obtained from *Iatrosophikon*, a recording of herbal prescriptions written during the Ottoman period (Lardos, 2006).

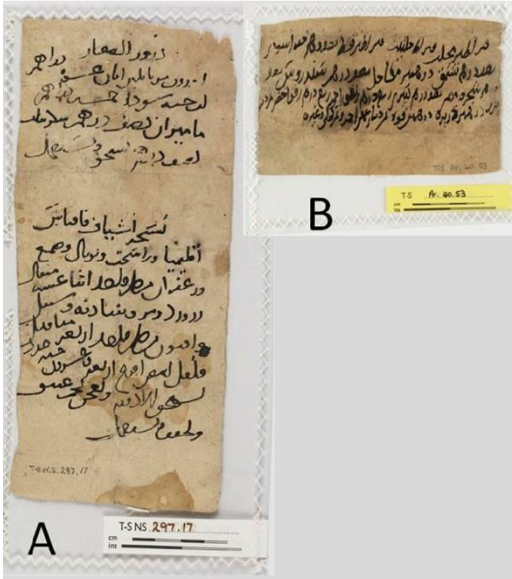

Figure 2.2. Collected remains of a medieval medical prescription written in Arabic from Cairo Genizah. A prescription for medicine containing *R. coriaria* might have looked similar to this (Botnick, 2012) ("Medieval practical medical prescriptions, found in the Cairo Genizah" by Botnick is licensed under CC BY 3.0).

Due to its many cited traditional uses, *R. coriaria* has been investigated for its possible antidiabetic, antimicrobial, and antioxidant characteristics. For example, previous studies show that *R. coriaria* exhibits various antidiabetic properties (Giancarlo, Rosa, Nadjafi, & Francesco, 2006) (Mohammadi, Montasser Kouhsari, & Monavar Feshani, 2010). Giancarlo et al. argued that the methanolic extract of the fruits have inhibitory activity against alpha-amylase, an enzyme involved in the metabolism of starch in humans, and so *R. coriaria* may be applied in therapy to treat hyperglycemia. Likewise, Mohammadi et al. showed that treatment of rats with the ethanolic fruit extract could decrease postprandial blood glucose in both short-term (5 hour) and long-term (21 day) assays by approximately 25%. *R. coriaria* has also been found to demonstrate antimicrobial activity, with documented inhibition against pathogens such as several *Bacillus*

species and *Proteus vulgaris* (Nasar-Abbas & Halkman, 2004). In addition, extracts of the plant have exhibited antioxidant properties, by showing activity against free radicals and lipid peroxidation (Bursal & Koksal, 2010; Candan & Sokmen, 2004).

2. *Rhus copallinum* L.

R. copallinum is commonly known by many names: dwarf sumac, winged sumac, flame leaf sumac, and shining sumac. The species is a shrub tree found in eastern North America, particularly in areas with dry soils on hillsides, in woodlands, and near roads (Elias, 1987). It bears seeds from October to December and flowers from July to September.

Figure 2.3. Dried leaves of *R. copallinum.* Pictured is a specimen of *R. copallinum* collected by Emory Herbarium members from Georgia, United States. The specimen can be viewed at the Emory University Herbarium.

The traditional uses of the plant are documented in a practical medicine book called *In the Practice of Medicine on Thomsonian Principles.* Written in 1850 by J.W. Comfort, the book was meant to serve as a household guide for treating certain ailments, from dysentery to skin infections. In a section titled "Upland Sumac (*Rhus glabrum*)," which is a species related to *R. copallinum* and *R. coriaria*, the author mentions a once common use of *R. copallinum*: "A strong decoction of the bark of the root of the dwarf sumac is employed as a sovereign remedy for venereal diseases, by the Chippewa Indians" (Comfort, 1850), who lived mostly in the northeastern region of the United States. A 1895 publication titled *Transactions of the Ohio State Eclectic Medical Association* more specifically documented the traditional uses of *R. copallinum*: "*R. copallinum* ... [was] used for like purposes while the first was valued by the Chippewa Indians in gonorrhea, and the gall-like excrescences on the leaves, powdered and made into an ointment, afforded the white settlers a remedy for piles" (Scudder, 1895). It is implied here that knowledge of the plant's medicinal applications was shared by the Native Americans with the New England settlers.

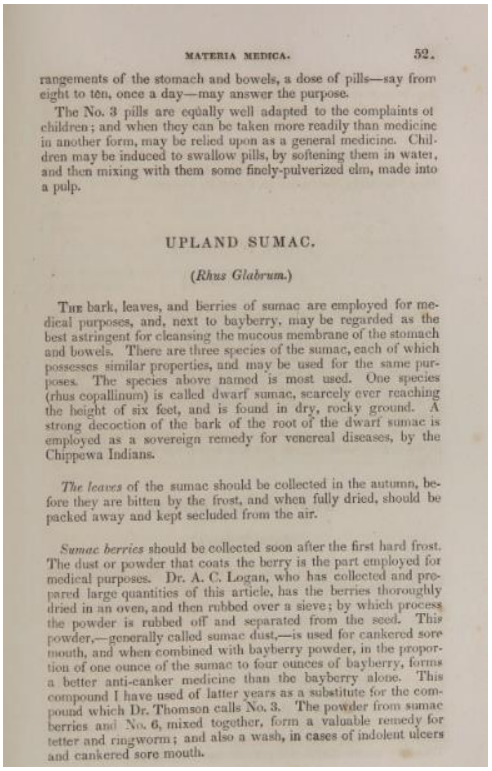

MATERIA MEDICA. 52.

rangements of the stomach and bowels, a dose of pills—say from eight to ten, once a day—may answer the purpose.

The No. 3 pills are equally well adapted to the complaints of children; and when they can be taken more readily than medicine in another form, may be relied upon as a general medicine. Children may be induced to swallow pills, by softening them in water, and then mixing with them some finely-pulverized elm, made into a pulp.

UPLAND SUMAC.

(*Rhus Glabrum.*)

The bark, leaves, and berries of sumac are employed for medical purposes, and, next to bayberry, may be regarded as the best astringent for cleansing the mucous membrane of the stomach and bowels. There are three species of the sumac, each of which possesses similar properties, and may be used for the same purposes. The species above named is most used. One species (rhus copallinum) is called dwarf sumac, scarcely ever reaching the height of six feet, and is found in dry, rocky ground. A strong decoction of the bark of the root of the dwarf sumac is employed as a sovereign remedy for venereal diseases, by the Chippewa Indians.

The leaves of the sumac should be collected in the autumn, before they are bitten by the frost, and when fully dried, should be packed away and kept secluded from the air.

Sumac berries should be collected soon after the first hard frost. The dust or powder that coats the berry is the part employed for medical purposes. Dr. A. C. Logan, who has collected and prepared large quantities of this article, has the berries thoroughly dried in an oven, and then rubbed over a sieve; by which process the powder is rubbed off and separated from the seed. This powder,—generally called sumac dust,—is used for cankered sore mouth, and when combined with bayberry powder, in the proportion of one ounce of the sumac to four ounces of bayberry, forms a better anti-canker medicine than the bayberry alone. This compound I have used of latter years as a substitute for the compound which Dr. Thomson calls No. 3. The powder from sumac berries and No. 6, mixed together, form a valuable remedy for tetter and ringworm; and also a wash, in cases of indolent ulcers and cankered sore mouth.

Figure 2.4. Excerpt from *In the Practice of Medicine on Thomsonian Principles* by J.W. Comfort. Page 52, here, offers practical uses of *R. glabrum* and *R. copallinum* to soothe venereal diseases (Comfort, 1850).

Previous studies on sifaka lemurs in captivity have shown a possible zoopharmacognosy aspect to the plant (Abhau, 2007). Zoopharmacognosy suggests that some non-human animals preferentially select certain plants and insects to guard against disease (Shurkin, 2014). Abhau documented *R. copallinum* leaves as a major staple in sifaka diets; sifakas preferentially select the plant amongst other foliage offerings throughout different seasons in the year. *R. copallinum* incorporation into the diets of captive sifakas has been associated with decreased incidence of diarrhea and overall balanced gastrointestinal systems (Abhau, 2007).

In addition to traditional literature, recent publications present the medicinal possibilities of *R. copallinum*. In a 2011 study on New England plants, *R. copallinum* displayed anticancer and antioxidant characteristics; fruit and leaf extracts of the plant inhibited two lines of human cancer colon cells (Ma, 2011). Another study isolated twelve compounds from the fruit of *R. copallinum*, including pentagalloyl glucose (PGG), a compound known for its antibacterial, antioxidant, anticarcinogenic, and anti-inflammatory properties (Ma et al., 2012) (Torres-León et al., 2017). Further research performed by the same leading author, Ma, showed that PGG isolated from fruit extracts of *R. copallinum* have antidiabetic properties too (Ma, Liu, Navindra, & Dain, 2014). Ma et al. showed that the extracts can decrease buildup of advanced glycation end products (AGEs) and inhibit albumin glycation, which are associated with diabetes.

CHAPTER 3: MATERIALS AND METHODS

Experimental overview

The goal of preliminary experimental procedures was to identify active plant materials that might prove effective against bacterial growth. To achieve this, our lab regularly performs bioactivity screens of the Quave Natural Product Library (QNPL), which contains traditional medicinal plants collected from private lands, conservatories, and parks around the world. When a particular plant extract is discovered through the screens to be active - as was the case with *Rhus coriaria*, *Rhus copallinum*, and *Schinus terebinthifolia*, further studies of the extract involve chemical analysis and microbiological validation. We follow the model of bio-guided fractionation, which involves continuously fractionating microbiologically active extracts via flash chromatography and High-Performance Liquid Chromatography (HPLC), in order to single out the active compound(s). Concurrent research in our lab resulted in the isolation of pentagalloyl glucose (PGG) from *S. terebinthifolia* (a member of the Anacardiaceae family). This Honors Thesis investigates PGG's activity against *Acinetobacter baumannii*, as well as PGG's presence in two related active plants in the QNPL, *R. coriaria* and *R. copallinum* (both in Anacardiaceae).

Preparing crude extract from plant material

1. Collections and processing -

   The leaves of *R. coriaria* were collected from Levanzo, Italy in June 2017, and the leaves of *R. copallinum* were collected from The Jones Center at Ichauway in Georgia, United States in July 2019, respectively. Voucher specimens were created for addition to the online and physical databases at Emory University Herbarium, where dried samples of intact plant parts may be retrieved for viewing. Plant parts collected for laboratory testing were

manually cleaned of contaminants, dried in low heat in a desiccating cabinet over several days, and then stored in sealed paper bags at room temperature. The samples were ground into coarse powder using a Wiley Mill plant grinder.

2. Extraction of organic phytochemicals –

Following a revised method of traditional maceration methods (NN, 2015), we performed a double maceration on the ground samples to release soluble phytochemicals. A single maceration step involved soaking the samples in alcohol for 72 hours, daily agitation via a stirring rod, and vacuum filtration (using coarse Fischer P8 paper and fine Fischer P2 paper for first and second filtrations, respectively) after the 72 hours. After the second maceration, the filtered samples were dried by rotary evaporation for solvent removal and then lyophilized for water removal. The crude extracts were stored at -20 °C. *R. coriaria*, which was macerated with 95% ethanol, was labeled as extract 1271. *R. copallinum*, which was macerated with 80% ethanol, was labeled as extract 1722.

Preparing extract partitions

1. Liquid-liquid partitioning –

The crude 1271 and 1722 extracts were partitioned via a modified Kupchan partitioning scheme into four partitions: hexane, ethyl acetate, n-butanol, and water partitions. These American Chemical Society grade solvents were purchased from Fisher Chemical. Crude extract was dissolved in a MeOH/dH_2O solution in a separatory funnel in a 1 gram: 30 mL solvent ratio. Hexane was added to the mixture at a volume of 1/3 of the total volume of dissolved extract solution, and the resultant organic layer was removed and filtered through anhydrous sodium sulfate. The hexane partitioning was performed two more times, for a total

of three times, to achieve the final hexane partition "B." We partitioned the ethyl acetate and then the water-saturated n-butanol layers in the same way, with three partitions for each solvent, to achieve the final ethyl acetate "C" and n-butanol "D" partitions. The remaining aqueous layer from the n-butanol partitions was not filtered through sodium sulfate; these aqueous volumes were combined to form our water "E" partition. All liquid partitions were concentrated by rotary evaporation. The C, D, and E partitions were then lyophilized while the B partition was dried via a Bar Vap evaporator. Percent yields for each partition were calculated, and partitions were stored at -20 °C.

Growth inhibition

1. Growth inhibition assays -

To determine the minimum inhibitory concentration (MIC) of extracts and antibiotics against bacterial strains, growth inhibition assays were performed via broth microdilution on sterile 96-well flat bottom, non-treated plates. All extract samples were dissolved at 10 mg/mL in DMSO (dimethyl sulfoxide) while antibiotics were dissolved at 10 mg/mL in dH_2O. The bacterial strain was plated onto Tryptic Soy Agar (TSA) from frozen stock and grown overnight in a 35 °C static incubator. To make an overnight (O/N) culture, a bacterial colony from the TSA plate was grown overnight in 6 mL of Tryptic Soy Broth (TSB) in a 35 °C shaking incubator. A Biotek Cytation 3 machine was used to standardize the O/N culture (now at logarithmic growth phase) to 5×10^5 colony-forming units/mL (optical density of 0.0006) to prepare the working culture (W/C) in cation-adjusted Mueller-Hinton Broth (CAMHB). Each condition was tested in triplicate. Extracts, vehicle (DMSO) control, and antibiotics (meropenem and/or gentamicin) were added to three wells at an initial concentration of 256 μg/mL. Three growth control wells were filled with 200 μL W/C

without any treatment, and three media blank wells were filled with 200 µL of CAMHB. W/C was added to the initial treatment wells and rest of the treatment wells to complete well volumes of 400 µL. The treatment wells were then diluted by two-fold serial dilution to final well volumes of 200 µL. The plate was incubated for 18 or 22 hours for non-*A. baumannii* and *A. baumannii* strains, respectively, in a 35 °C static incubator. Initial (0-hour) and 22-hour plate reads were performed on the Biotek Cytation 3 machine, and growth inhibition of each treatment was calculated with the following equation.

$$\%\ growth\ inhibition = [1\ -\ (\frac{ODt22\ -\ ODt0}{avg(ODvc22\ -\ ODvc0}})]\ \times\ 100$$

ODt0: OD_{600nm} for the extract treatment at 0-hour
ODt22: OD_{600nm} for the extract treatment at 22-hour post-incubation
ODvc0: OD_{600nm} for the vehicle control (DMSO treatment) at 0-hour
ODvc22: OD_{600nm} for the vehicle control (DMSO treatment) at 22-hour post-incubation

Averages and standard deviations of the percent growth inhibitions of each treatment were calculated. The MIC (where ≥ 90% of bacterial growth was inhibited) and IC_{50} (where ≥ 50% of bacterial growth was inhibited) were determined by the averages of each treatment.

a. Assay types: Growth inhibition assays were performed for a panel of 7 *A. baumannii* strains (Table 3.2) against the extracts 1271, 1271B, 1271C, 1271D, and 1271E. Assays were also performed on 1271C, 1722C, and pure PGG against the ESKAPE panel. The ESKAPE panel consisted of multidrug resistant bacteria: *Enterococcus faecium, Staphylococcus aureus, Klebsiella pneumoniae, Acinetobacter baumannii, Pseudomonas aeruginosa, and Enterobacter* spp (Table 3.1). In addition, assays were performed on pure PGG (purchased from Sigma-Aldrich) against a library of 24 *A. baumannii* strains that have varying resistance profiles (Table 3.2). The

growth inhibition assay for *A. baumannii* AB5075 against PGG was performed in both CAMHB and TSB.

Species	Strain ID	Alternate ID	Antibiotic resistance profile	Characteristics of strain	Other information
Acinetobacter baumannii	AB5075		Amk^R, Sam^R, Fep^R, Caz^R, Cip^R, Gen^R, Ipm^R, Mem^R, Tet^S, Tob^R		Laboratory strain. Sequencing information: GenBank#: GCA_000770605.1. Providing source: Phil Rather.
	ATCC17978				Clinical isolate from infant with fatal meningitis. Sequencing information: Nucleotide (GenBank): CP000521. Providing source: Phil Rather.
Enterobacter cloacae	CDC-32	AR-BANK #0032	Amk^S, Sam^R, Fep^R, Caz^R, Cip^S, Dor^I, Gen^R, Ipm^R, Mem^R, Tet^S, Tob^I	Reduced susceptibility, elevated Carbapenem MICs. Known acquired resistance: KPC-3, TEM-1.	Clinical isolate. Providing source: CDC AR Bank.
Enterococcus faecium	EU-44	HM-959; Strain 513			Providing source: BEI Resources.
Klebsiella pneumoniae	EU-32	NR-15410		Contains the β-lactamase *K. pneumoniae* carbapenemase (blaKPC) gene.	Providing source: BEI Resources.
Pseudomonas aeruginosa	AH-0071	PAO1			Laboratory strain. Providing source: Alex Horswill.
Staphylococcus aureus	AH-1263		Ery^S, Oxa^R		Laboratory strain. Providing source: Alex Horswill.

Table 3.1. Pathogenic ESKAPE strains that were tested in growth inhibition assays of PGG, 1271C, and 1722C. The antibiotic resistance profiles and strain characteristics were reported by

the source provider. Abbreviations for antibiotics are listed: amikacin (Amk), ampicillin/sulbactam (Sam), cefepime (Fep), ceftazidime (Caz), ciprofloxacin (Cip), colistin (Cst), doripenem (Dor), erythromycin (Ery), gentamicin (Gen), imipenem (Ipm), oxacillin (O), polymyxin B (Pmb), tetracycline (Tet), and tobramycin (Tob). Abbreviations for antibiotic resistance are represented as superscripts: R for resistant, S for susceptible, and I for intermediate. S-I-R interpretation is based on CLSI (Clinical and Laboratory Standards Institute) guidelines (Cockerill, 2013).

Strain ID	Alternate ID	Antibiotic resistance profile	Characteristics of strain	Other information
AB5075		Amk^{R},Sam^{R},Fep^{R},Caz^{R},Cip^{R},Gen^{R},Ipm^{R},Mem^{R},Tet^{S},Tob^{R}		Laboratory strain. Sequencing information: GenBank#: GCA_000770605.1. Providing source: Phil Rather.
ATCC17978				Clinical isolate from infant with fatal meningitis. Sequencing information: Nucleotide (GenBank): CP000521. Providing source: Phil Rather.
CDC-33	AR-BANK#0033	Amk^{S},Sam^{R},Fep^{R},Caz^{R},Cip^{R},Cst^{S},Gen^{R},Ipm^{R},Mem^{R},Tet^{S},Tob^{R}	Reduced susceptibility, elevated Carbapenem MICs. Known acquired resistance: NDM-1.	Providing source: CDC AR Bank.
CDC-35	AR-BANK#0035	Amk^{S},Sam^{R},Fep^{R},Caz^{R},Cip^{R},Cst^{S},Gen^{R},Ipm^{R},Mem^{R},Tet^{R},Tob^{S}	Reduced susceptibility, elevated Carbapenem MICs. Known acquired resistance: OXA-72.	Providing source: CDC AR Bank.
CDC-36	AR-BANK#0036	Amk^{I},Sam^{I},Fep^{R},Caz^{R},Cip^{R},Cst^{S},Gen^{I},Ipm^{R},Mem^{R},Tet^{R},Tob^{R}	Reduced susceptibility, elevated Carbapenem MICs. Known acquired resistance: OXA-24, OXA-40.	Providing source: CDC AR Bank.
CDC-37	AR-BANK#0037	Amk^{S},Sam^{R},Fep^{R},Caz^{R},Cip^{R},Cst^{S},Gen^{R},Ipm^{R},Mem^{R},Tet^{S},Tob^{R}	Reduced susceptibility, elevated Carbapenem MICs. Known acquired resistance: NDM-1.	Providing source: CDC AR Bank.

CDC-45	AR-BANK#0045	Amk^{S},Sam^{R},Fep^{R},Caz^{R},Cip^{R},Cst^{S},Gen^{R},Ipm^{R},Mem^{R},Tet^{R},Tob^{S}	Reduced susceptibility, elevated Carbapenem MICs. Known acquired resistance: OXA-23.	Providing source: CDC AR Bank.
CDC-52	AR-BANK#0052	Ank^{S}, Sam^{S}, Fep^{S}, Caz^{S}, Ctx^{R}, Cip^{R}, Cst^{S}, Cro^{R}, Dor^{R},Gen^{R}, Ipm^{R}, Mem^{R}, Lvx^{R}, Pmb^{S}, Tet^{S}, Tzp^{R}, Tob^{R}, Sxt^{R},	Reduced susceptibility, elevated Carbapenem MICs. Known acquired resistance: OXA-58.	Providing source: CDC AR Bank.
CDC-70	AR-BANK#0070	Amk^{S},Sam^{S},Fep^{S},Caz^{I},Cip^{R},Cst^{S},Gen^{R},Ipm^{R},Mem^{R},Tet^{S},Tob^{R}	Reduced susceptibility, elevated Carbapenem MICs. Known acquired resistance: OXA-58.	Providing source: CDC AR Bank.
CDC-102	AR-BANK#0102	Amk^{R},Sam^{S},Fep^{R},Caz^{R},Cip^{R},Cst^{S},Gen^{R},Ipm^{S},Mem^{I},Tet^{S},Tob^{R}	Reduced susceptibility, elevated Carbapenem MICs. No known acquired resistance.	Providing source: CDC AR Bank.
CDC-273	AR-BANK#0273	Amk^{R},Sam^{R},Fep^{R},Caz^{R},Cip^{R},Cst^{S},Gen^{R},Ipm^{R},Mem^{R},Tet^{R},Tob^{R}		Providing source: CDC AR Bank.
CDC-274	AR-BANK#0274	Amk^{S},Sam^{R},Fep^{R},Caz^{R},Cip^{R},Cst^{S},Gen^{R},Ipm^{R},Mem^{R},Tet^{R},Tob^{S}		Providing source: CDC AR Bank.
CDC-275	AR-BANK#0275	Amk^{R},Sam^{R},Fep^{R},Caz^{R},Cip^{R},Cst^{S},Gen^{R},Ipm^{R},Mem^{R},Tet^{R},Tob^{R}		Providing source: CDC AR Bank.
CDC-277	AR-BANK#0277	Amk^{S},Sam^{R},Fep^{R},Caz^{R},Cip^{R},Gen^{R},Ipm^{R},Mem^{R},Tet^{R},Tob^{R}		Providing source: CDC AR Bank.
CDC-278	AR-BANK#0278	Amk^{R},Sam^{R},Fep^{R},Caz^{R},Cip^{R},Cst^{S},Gen^{R},Ipm^{R},Mem^{R},Tet^{R},Tob^{R}		Providing source: CDC AR Bank.
CDC-281	AR-BANK#0281	Amk^{S},Sam^{R},Fep^{I},Caz^{R},Cip^{R},Cst^{S},Gen^{R},Ipm^{R},Mem^{R},Tet^{R},Tob^{S}		Providing source: CDC AR Bank.
CDC-282	AR-BANK#0282	Amk^{R},Sam^{R},Fep^{R},Caz^{R},Cip^{R},Cst^{S},Gen^{R},Ipm^{R},Mem^{R},Tet^{R},Tob^{R}		Providing source: CDC AR Bank.
CDC-283	AR-BANK#0283	Amk^{R},Sam^{R},Fep^{R},Caz^{R},Cip^{R},Cst^{S},Gen^{R},		Providing source: CDC AR Bank.

		Ipm^{R},Mem^{R},Tet^{R},Tob^{R}		
CDC-284	AR-BANK#0284	Amk^{R},Sam^{R},Fep^{R},Caz^{R},Cip^{R},Cst^{S},Gen^{R},Ipm^{R},Mem^{R},Tet^{R},Tob^{R}		Providing source: CDC AR Bank.
CDC-295	AR-BANK#0295	Amk^{S},Sam^{R},Fep^{R},Caz^{R},Cip^{R},Cst^{S},Gen^{S},Ipm^{R},Mem^{R},Tet^{R},Tob^{S}		Providing source: CDC AR Bank.
CDC-299	AR-BANK#0299	Amk^{R},Sam^{R},Fep^{R},Caz^{R},Cip^{R},Cst^{S},Gen^{R},Ipm^{R},Mem^{R},Tet^{R},Tob^{R}		Providing source: CDC AR Bank.
CDC-300	AR Bank #0300	Amk^{R},Sam^{S},Fep^{I},Caz^{R},Cip^{R},Cst^{S},Gen^{R},Ipm^{S},Mem^{S},Tet^{R},Tob^{R}		Providing source: CDC AR Bank.
EU-24	Naval-81; NR-17786	Gen^{I}		Clinical isolate from human blood. Sequencing information: genome sequence at GenBank: AFDB00000000.Providing source: BEI Resources.
EU-27	OIFC143; 5-143; NR-17781			Clinical isolate from thigh wound. Providing source: BEI Resources.
EU-35	NR-9667			Isolated from sputum of injured soldier. Providing source: BEI Resources.

Table 3.2. Twenty-five *A. baumannii* strains used in growth inhibition assays. The antibiotic resistance profiles and strain characteristics were reported by the source provider. Abbreviations for antibiotics are listed: amikacin (Amk), ampicillin/sulbactam (Sam), cefepime (Fep), ceftazidime (Caz), ciprofloxacin (Cip), colistin (Cst), doripenem (Dor), erythromycin (Ery), gentamicin (Gen), imipenem (Ipm), oxacillin (O), polymyxin B (Pmb), tetracycline (Tet), and tobramycin (Tob). Abbreviations for antibiotic resistance are represented as superscripts: R for resistant, S for susceptible, and I for intermediate. S-I-R interpretation is based on CLSI (Clinical and Laboratory Standards Institute) guidelines (Cockerill, 2013).
The strains highlighted in red were included in the growth inhibition assays of 1271 partitions against the 7 *A. baumannii* strains. All strains listed here, except CDC-52, were in the growth inhibition assays of PGG against the 24 *Acinetobacter baumannii* strains.

Supplementation studies

1. Iron supplementation assays

Growth inhibition assays with iron supplementation were performed to determine the possible effect of iron on PGG's mechanism of inhibition. For this assay, the growth inhibition procedure was performed on two plate conditions: control plate and iron supplementation plate. The control plate tested PGG against strain AB5075 (a highly resistant *A. baumannii* strain) using regularly prepared CAMHB. The supplementation plate used CAMHB supplemented with 1 mM of iron (II) sulfate (purchased from VWR). Percent inhibitions and MIC considerations were calculated as previously described, and the control plate and supplementation plates were compared for effect of iron on PGG's mechanism of action. This iron supplementation assay was also performed for iron (III) sulfate (purchased from VWR).

Growth inhibition assays were also performed in iron-depleted CAMHB, using the same procedure as previously described in the "Growth inhibition" section. To prepare the iron-depleted CAMHB, a mixture of Chelex 100 Chelating Resin (purchased from Bio-Rad), CAMHB powder, and dH_2O was prepared according to the manufacturer's directions. Following an hour of stirring, the solution was sterile-filtered through a bottle-top vacuum filter. The resulting iron-depleted broth was utilized for both the overnight and working cultures.

2. Lipid supplementation assays

Growth inhibition assays with lipid supplementation were performed to determine the possible effect of lipids on PGG's mechanism of inhibition. The same procedure used for iron supplementation assays was performed. Two supplementation plate conditions were performed: CAMHB supplemented with 0.02% w/v oleic acid and CAMHB supplemented with 0.02% w/v polysorbate 80 (TWEEN 80 from Sigma-Aldrich).

3. Optical density of PGG with iron supplementation

The visual effect of iron supplementation on PGG was quantified on a Cytation 3 multimode plate reader (Biotek®, Winooski, VT, United States) by optical density (OD_{590nm}) readings. Iron (II) sulfate ($FeSO_4$) and iron (III) sulfate hydrate ($Fe_2(SO_4)_3xH_2O$) were dissolved at 10 mg/mL in dH_2O and then added to CAMHB for a final concentration of 1mM of iron. Each iron-supplemented medium was added to a 96-well non-tissue culture treated plate in triplicate rows. PGG stock (Sigma-Aldrich) was dissolved at 10 mg/mL in DMSO and added to the 96-well plate in a two-fold serial dilution, with triplicate rows ranging from 512 μg/mL to 16 μg/mL of PGG, for the triplicate rows of iron (II) supplemented media, iron (III) supplemented media, and CAMHB alone. Control wells for iron (II) supplemented media, iron (III) supplemented media, and CAMHB alone were plated in triplicates as well. The optical density of the 96-well plate was quantified at 0 hours and 24 hours after plating.

Biofilm studies

1. Biofilm formation inhibition -

To assess whether PGG might inhibit biofilm formation of *A. baumannii*, a biofilm formation inhibition assay was performed on *A. baumannii* AB5075 against PGG on a 96-well flat bottom plate. This assay was modified from the methods of earlier *A. baumannii* literature (Tipton, Dimitrova, & Rather, 2015). Overnight culture of *A. baumannii* AB5075 was standardized to 5 x 10^5 CFU/mL in Luria-Bertani (LB) (supplemented with 2% dextrose) using a Cytation 3 multimode plate reader (Biotek®, Winooski, VT, United States) at OD_{600nm} to create working culture. The highest concentration of PGG was subIC_{50}, which was defined as the concentration below the $IC_{50.}$ Concentrations of DMSO, PGG, and tetracycline were added to the corresponding

wells at a 2-fold serial dilution: while DMSO and PGG wells ranged from 4 µg/mL to 0.313 µg/mL, the tetracycline wells ranged from 64 µg/mL to 0.5 µg/mL. The plate was incubated statically at 35°C for 22 hours, and optical density readings (600nm) of the plate were performed at 0 hours and 22 hours after incubation. After 22 hours of incubation, the plate was stained with crystal violet, rinsed with tap water, and left to dry. Once the plate was dry, a picture of the stained plate was captured. The plate was eluted with 10% of 2.5% TWEEN 80 (polysorbate 80) in ethanol, and the eluate was transferred to a plate with 1 x PBS (phosphate-buffered saline) in a 10-fold dilution. The optical density (595nm) of the plate was read, and the %inhibition was determined using the following formula.

$$\%\ inhibition = [1\ -\ (\frac{ODt}{avg(ODvc)})]\ \times\ 100$$

ODt: OD_{595nm} for the extract treatment
ODvc: OD_{595nm} for the vehicle treatment

The $MBIC_{90}$ (where ≥ 90% of biofilm formation was inhibited) and $MBIC_{50}$ (where ≥ 50% of biofilm formation was inhibited) were determined by the averages of each treatment.

2. Biofilm eradication -

To assess whether PGG might eradicate the biofilm of *A. baumannii*, a biofilm eradication assay was performed on *A. baumannii* AB5075 against PGG on a 96-well flat bottom plate. This assay was modified from the methods of earlier *A. baumannii* literature (Tipton et al., 2015). Overnight culture of *A. baumannii* AB5075 was standardized to 5 x 10^5 CFU/mL in LB media (supplemented with 2% dextrose) using a Cytation 3 multimode plate reader (Biotek®, Winooski, VT, United States) at OD_{600nm} to create working culture. For a "formed biofilm plate", working culture was added to all wells, except for media blank wells, which received LB media (supplemented with 2% dextrose). The plate was incubated statically at 35°C for 22 hours, and optical density readings

(600nm) of the plate were performed at 0 hours and 22 hours after incubation. Before the 22-hour timepoint, a separate "biofilm treatment plate" was created with fresh LB and treatments. For this plate, concentrations of DMSO, PGG, and tetracycline were added to the corresponding wells at a 2-fold serial dilution: while DMSO and PGG wells ranged from 256 µg/mL to 2 µg/mL, the tetracycline wells ranged from 512 µg/mL to 4 µg/mL. At the 22-hour timepoint, optical density of the "formed biofilm plate" was measured, and then media in this plate was removed. Media from the "biofilm treatment plate" was transferred to the "formed biofilm plate", and optical density readings were performed on the "formed biofilm plate" again. The plate was incubated statically at 35°C for another 22 hours, after which the optical density of the plate was read. The plate was then stained with crystal violet, rinsed with tap water, and left to dry. Once the plate was dry, a picture of the stained plate was captured. The plate was eluted with 10% of 2.5% TWEEN 80 (polysorbate 80) in ethanol, and the eluate was transferred to a plate with 1xPBS in a 10-fold dilution. The optical density (595nm) of the plate was read, and the %inhibition was determined using the following formula.

$$\%\ eradication = [1\ -\ (\frac{ODt}{avg(ODvc)})]\ \times\ 100$$

ODt: OD_{595nm} for the extract treatment
ODvc: OD_{595nm} for the vehicle treatment

The $MBEC_{90}$ (where ≥ 90% of biofilm was eradicated) and $MBEC_{50}$ (where ≥ 50% of biofilm was eradicated) were determined by the averages of each treatment.

Time-kill assays

An overnight culture of *A. baumannii* AB5075 was prepared in TSB. After overnight incubation (35°C), a working culture was prepared in CAMHB by standardizing the overnight culture to 5 x 10^5 colony-forming units/mL. A total of five conditions were tested: DMSO, PGG alone, PGG with 0.02% oleic acid supplementation, PGG with 0.02% polysorbate 80 supplementation, and PGG with 1 mM of iron (II) sulfate supplementation. Four replicates of each condition were included for the following plate. In a 96-well plate, PGG and vehicle (DMSO) control were added to working culture at concentrations of 256 µg/mL. Oleic acid, polysorbate 80, and iron (II) sulfate were added to the corresponding wells at concentrations of 0.02%, 0.02%, and 1 mM, respectively. The remaining procedures (dilution and spotting agar) were performed at the following time points: 0, 3, 6, and 24 hours.

At each timepoint, each treatment was serially diluted 10-fold in sterile PBS and 10 µL of each dilution was spotted on TSA plates. The numbers of colonies in each spot on the agar were counted, and the numbers of colony-forming units per mL (CFU/mL) of the original bacterial culture were calculated for each condition.

Resistance studies

1. Spontaneous mutant assay

Spontaneous mutant assays were performed for *A. baumannii* AB5075 to observe for possible development of spontaneous mutants after interaction with PGG, and to confirm an effect of iron on PGG activity. Assays were performed in TSA on 6 cm Petri plates, and then twice in both cation-adjusted Mueller-Hinton Agar (CAMHA) and TSA on 96-well plates. For the first half of the assay, PGG was mixed with agar solution at concentrations of 0.5 x MIC, 1 x MIC, and 2 x MIC (128, 256, and 512 µg/mL, respectively). Previous determination of the MIC of PGG against AB5075 was applied here. A control condition with no PGG treatment was included for each assay.

For the 96-well assay, each condition was tested in triplicate, and media blank wells were included for each condition. Overnight culture of *A. baumannii* AB5075 was standardized to 5 x 10^5 CFU/mL in CAMHB media using a Cytation 3 multimode plate reader (Biotek®, Winooski, VT, United States) at $OD_{600nm.}$ AB5075 working culture was spread onto each treatment plate, statically incubated at 35 °C for 24 hours, and observed for presence of bacterial growth and color of agar. At the 24-hour mark, 1mM of iron (II) sulfate solution or 1 mM of iron (III) sulfate solution was spread onto the agar; iron solution was added to the 0.5 x MIC and 2 x MIC plates for the Petri plate assay, and to all of the PGG-treated wells for the 96-well assay. The plates were statically incubated at 35 °C. The plates were visually observed for presence of bacterial growth at 24 and 48 hour timepoints.

2. Resistance development through serial passaging

The resistance profile of *A. baumannii* AB5075 against PGG was further characterized by a 21-day serial passaging assay of AB5075 against sub-MIC (sub-inhibitory) concentrations of PGG. The serial resistance passaging experiment was modified from previous literature (Wang et al., 2018). Each passage plate was plated according to CLSI guidelines for broth microdilution growth inhibition assays, with some modifications (Cockerill, 2013). Each passage was performed on a 96-well non-tissue culture treated plate, with PGG, vehicle (DMSO) control, and antibiotic control (tetracycline) added in two-fold serial dilution across a range of eight concentrations. All concentrations were tested in triplicates, and additional control wells included growth control (AB5075 working culture) and media blank (CAMHB). Each plate was statically incubated at 35 °C for 20 - 24 hours, as per CLSI guidelines, in between serial passages.

For the first plate, overnight culture of *A. baumannii* AB5075 was standardized to 5 x 10^5 CFU/mL in CAMHB media using a Cytation 3 multimode plate reader (Biotek®, Winooski, VT, United States) at $OD_{600nm.}$ The following eight concentration ranges were tested for the first plate: 512 - 4 μg/mL PGG, 512 - 4 μg/mL DMSO, and 64 - 0.5 μg/mL tetracycline.

For the next 20 days, serial passaging was performed by reading the OD_{600nm} of the previous day's plate and calculating the percent growth inhibitions as previous described in the "Growth inhibition" section. The IC_{50} and MIC were determined as the concentration at which there is 50% and 90% growth inhibition, and the sub-MIC was defined as 0.5 x MIC. The subsequent working cultures of PGG-treated bacteria and tetracycline-treated bacteria were made by taking bacterial solution from the most turbid well (OD_{600nm}) of the respective sub-MIC triplicates from the previous day's plate and diluted to 5 x 10^5 CFU/mL in CAMHB. The same plating procedure from day 1 was followed for each day, except with the sub-MIC working cultures.

Cytotoxicity assays

Cytotoxicity assays of immortalized human keratinocytes (HaCaTs) were performed using a lactate dehydrogenase (LDH) cytotoxicity assay kit (G-Biosciences, St. Louis, MO). The procedure was performed according to the manufacturer's instructions. The HaCaTs were maintained in Dulbeco's Modified Eagle Medium (DMEM) with 4.5 g/L glucose and L-glutamine. For the assay, the cells were standardized to 4 x 10^4 cells per mL, using a hemocytometer to count the number of suspended colonies. In order to seed the cells in a 96-well culture treated plate, 200 μL of working culture was transferred to each well, and the plate was incubated in a humidified incubator for 48 hours in 5% $CO_{2,}$ at 37 °C. After 48 hours, the medium in the plate was replaced with fresh medium. Extract treatment (previously sterile filtered) was added to wells in a gradient

of 256 µg/mL to 32 µg/mL. After 23 hours and 15 minutes of incubation (5% CO_2, at 37 °C), lysis buffer was transferred to the positive control on the plate, so that the optical density of complete cell lysis could be obtained. The plate was incubated for 45 minutes, rounding the total plate incubation to 24 hours of treatment. Then, the plate was centrifuged at 1500 rpm for 5 minutes, and the resulting supernatant was transferred to a separate plate containing Substrate Mix and Assay Buffer (provided in the G-Biosciences LDH kit). After 20 minutes of incubation at 37 °C, Stop Solution (provided in the G-Biosciences LDH kit) was added to the wells. Then, optical density measurements (490 nm) were performed on the plate. The percent cytotoxicity was calculated using the following formula, which was provided by the kit's manufacturer.

$$\%\ cytotoxicity = \left(\frac{ODt - avg(ODs)}{avg(ODm)}\right) \times 100$$

ODt: OD_{490nm} for the extract treatment
ODs: OD_{490nm} for the spontaneous control
ODm: OD_{490nm} for the maximum control

The IC_{50} (where ≥ 50% of growth was inhibited) was determined by the averages of each treatment.

Using HPLC as a means of detection and quantification

1. Analytical HPLC -

Analytical High-Performance Liquid Chromatography was used for chemical analysis of partition components by separating solutes by their relative polarities. The stationary phase consisted of an Agilent Eclipse XDB-C18 4.6*250 mm, 5 µm column, and the mobile phase (HPLC-grade

solvents from Fisher Scientific) consisted of a gradient system of two solvents supplemented with formic acid.

2. Co-injection studies -

Co-injection studies were performed for detection of PGG in extracts 1271C and 1722C, at a column temperature of 40 °C. Extract samples for HPLC injection were dissolved at 10 mg/mL in MeOH. PGG samples were dissolved at 1mg/mL in MeOH. Co-injection samples of extract plus PGG were mixed in a 9:1 (extract: PGG) ratio. The mobile phase consisted of (A) 0.1% (vol/vol) formic acid in water and (B) 0.1% (vol/vol) formic acid in methanol at a flow rate of 1.0 mL/min. Initial conditions were 70:30 (A: B), changing to 65:35 (A: B) at 7 minutes, then to 60:40 (A: B) at 13 minutes, then to 0:100 (A: B) at 20 minutes, and finally to 70:30 (A: B) at 30 minutes. The 70:30 (A: B) gradient was held until 40 minutes. Chromatograms of each sample were compared to the chromatogram of the PGG sample (at 217 nm) to identify the possible PGG peak in the extracts.

CHAPTER 4: RESULTS

Extraction and liquid-liquid partitioning

An initial growth inhibition screen of the Quave Natural Product Library (QNPL) revealed extracts 1271 (*Rhus coriaria* leaves) and 1722 (*Rhus copallinum* leaves) to be active against *Acinetobacter baumannii* (> 80% growth inhibition at 256 µg/mL). Figure 4.1 shows the pathway of bio-guided fractionation that was followed for crude 1271, as well as the percent yields of each partition. The total percent yield of the 1271 liquid-liquid partitioning was 96.22%, indicating a loss of 3.78% of the original extract 1271. The partitioning of 1722 was performed previously in our lab.

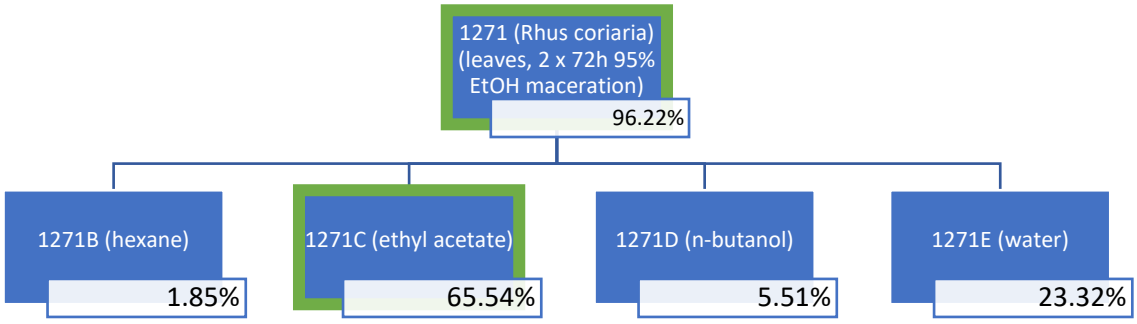

Figure 4.1. Partition scheme of 1271. Percent yields are listed below each partition. The highlighted green boxes indicate the most active extracts selected for the next step of bio-guided fractionation.

Growth inhibition assays

Preliminary MICs of 1271 fractions

Preliminary growth inhibition assays reveal 1271C (ethyl acetate partition) to be the most active partition against a panel of seven *A. baumannii* strains. The IC_{50} and MIC are presented in

Table 4.1, and the growth inhibition curves are presented in Figure 4.2. The resistance profiles and characteristics differ between the selected strains, and the defining characteristics of each strain are presented in Table 3.2 in Methods.

	ATCC17978		AB5075		CDC33		CDC35		CDC36		CDC45		CDC52	
	IC50	MIC	IC50	MIC	IC50	MIC	IC50	MIC	IC50	MIC	IC50	MIC	IC50	MIC
1271	16	256	32	256	32	256	32	-	32	-	32	256	64	-
1271B	-	-	-	-	-	-	-	-	-	-	-	-	-	-
1271C	<8	256	16	256	16	256	16	256	16	256	16	128	32	256
1271D	16	-	32	-	32	-	32	-	32	-	32	256	32	-
1271E	-	-	-	-	-	-	-	-	-	-	-	-	-	-
Mem	<8	<8	<64	64	-	-	-	-	128	256	64	128	<8	<8
Gen	<8	<8	-	-	32	-	16	32	8	32	64	-	8	32

Table 4.1. IC_{50} and MIC values of growth inhibition assays of 1271 partitions against *A. baumannii* strains. These values represent the concentration (μg/mL) of extract or antibiotic needed to inhibit 50% and 90% of bacterial growth, relative to the vehicle (DMSO) control. "-" indicates that the value was not detected at the tested concentrations of 0-256 μg/mL for extracts and meropenem (Mem), or 2-64 μg/mL for gentamicin (Gen), indicating that the value is above the tested concentrations.

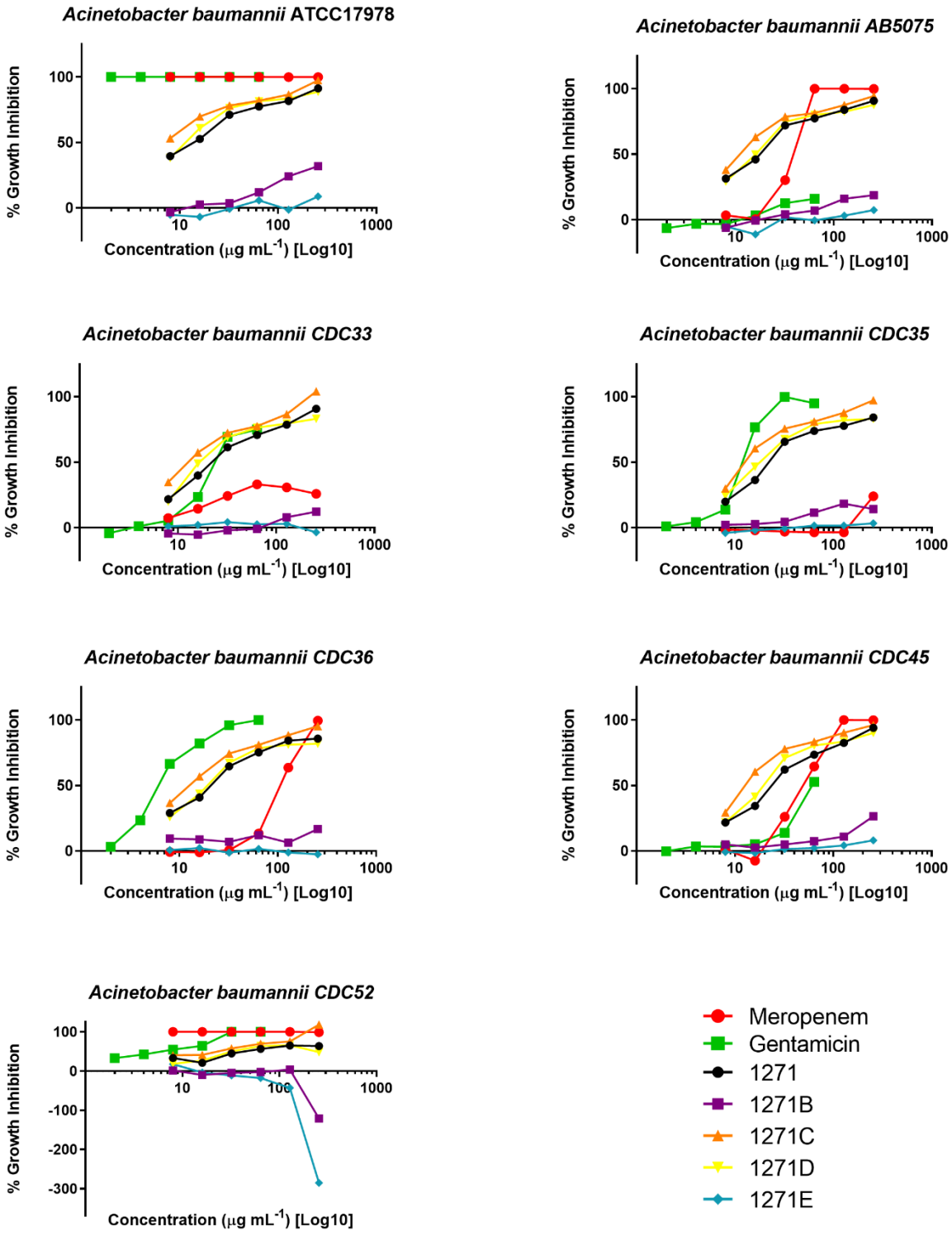

Figure 4.2. Growth inhibitions of a panel of *A. baumannii* strains by 1271 fractions. Due to the variance in resistance profiles among strains in the panel, two positive antibiotic controls (meropenem and gentamicin) were used. Data represent percent growth inhibition relative to the vehicle (DMSO) control.

Pentagalloyl glucose (PGG) and active *Rhus* fractions against ESKAPE panel

Growth inhibition assays of PGG and the active *Rhus* fractions (1271C and 1722C) were performed against bacterial strains from the pathogenic "ESKAPE" panel. The characteristics of each strain selected for testing from the ESKAPE panel are presented in Table 3.1. in Methods. The percent inhibition curves of PGG, 1271C, and 1722C are comparative for all of the strains tested. Table 4.2 below presents the individual IC_{50} and MIC values for PGG, 1271C, 1722C, and the antibiotic control against each strain, and Figure 4.3 includes the growth inhibition curves.

		PGG		1271C		1722C		Mem	
		IC50	MIC	IC50	MIC	IC50	MIC	IC50	MIC
Gram-positive	*Enterococcus faecium* EU-44	32	64	32	128	-	-	<0.125	-
	Staphylococcus aureus AH-1263	16	64	32	64	64	256	1	4
Gram-negative	*Acinetobacter baumannii* ATCC17978	8	64	16	128	32	128	<0.125	0.25
	Acinetobacter baumannii AB5075	8	64	16	128	32	128	32	64
	Enterobacter cloacae CDC-32	32	-	32	-	64	-	<0.125	16
	Klebsiella pneumoniae EU-32	16	-	32	-	64	-	256	-
	Pseudomonas aeruginosa AH-0071	4	16	8	32	16	64	1	2

Table 4.2. IC_{50} and MIC values of growth inhibition assays of extracts against ESKAPE panel pathogens. These values represent the concentration (μg/mL) of extract or antibiotic needed to inhibit 50% and 90% of bacterial growth, relative to the vehicle (DMSO) control. "-" indicates that the value was not detected at the tested concentrations of 0.125-256 μg/mL for extracts and meropenem (Mem), indicating that the value is above the tested concentrations.

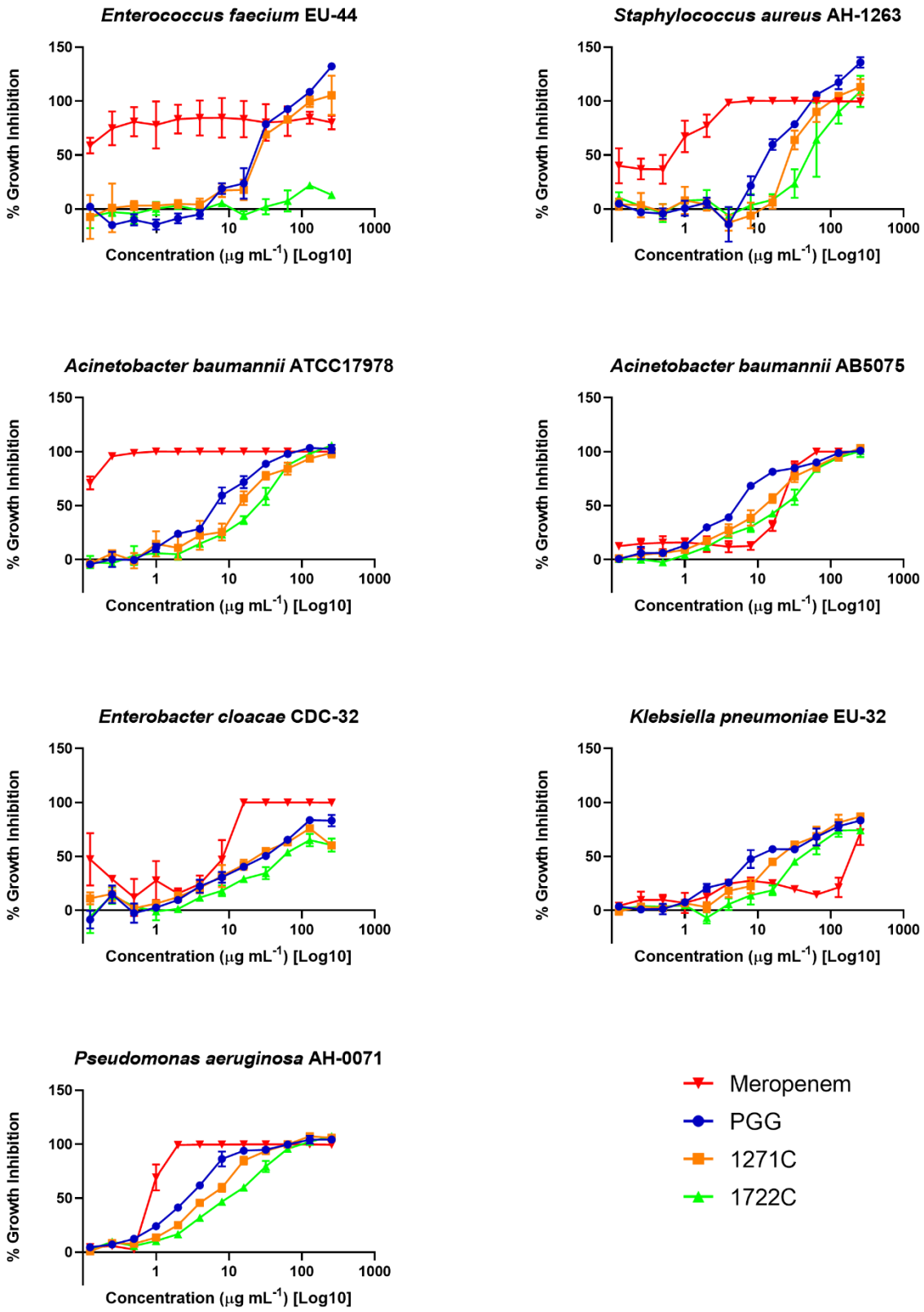

Figure 4.3. Growth inhibition of seven ESKAPE pathogens tested against PGG, 1271C, and 1722C. The curves represent percent growth inhibition relative to the vehicle (DMSO) control.

PGG against *A. baumannii* panel

A total of twenty-four *A. baumannii* strains were tested against PGG, with colistin and meropenem used as positive antibiotic controls. The resistance profiles and characteristics differ between the selected strains, and the defining characteristics of each strain are presented in Table 3.2 in Methods. Figure 4.4 captures the dose-response curve of each strain on a Log10 scale. The curves show an increase in percent growth inhibition with increasing concentrations of PGG. Table 4.3 shows the individual IC_{50} and MIC values for PGG and the antibiotic controls against each strain.

	PGG		Mem		Cst	
	IC50	MIC	IC50	MIC	IC50	MIC
EU-24	8	-	<2	4	<0.5	<0.5
EU-27	4	256	<2	<2	<0.5	<0.5
EU-35	16	256	-	-	<0.5	<0.5
CDC-33	8	-	-	-	<0.5	<0.5
CDC-35	8	256	-	-	<0.5	<0.5
CDC-36	16	-	-	-	<0.5	<0.5
CDC-37	8	256	-	-	<0.5	<0.5
CDC-45	8	256	-	-	<0.5	<0.5
CDC-70	16	-	4-8	8	<0.5	<0.5
CDC-102	8	-	<2	4	<0.5	<0.5
CDC-273	8	128	-	-	<0.5	<0.5
CDC-274	8	256	-	-	<0.5	<0.5
CDC-275	8	-	-	-	<0.5	<0.5
CDC-277	8	128	-	-	<0.5	<0.5
CDC-278	8	256	-	-	<0.5	1
CDC-281	8	128	-	-	<0.5	1
CDC-282	16	-	-	-	<0.5	<0.5
CDC-283	8	128	-	-	0.5-1	1
CDC-284	8	128	-	-	<0.5	<0.5
CDC-295	8	256	-	-	<0.5	<0.5
CDC-299	8	256	-	-	1-2	2
CDC-300	8	128	<2	4	1	2
AB5075	8	256	-	-	0.5-1	1
ATCC17978	8	256	<2	<2	<0.5	<0.5

Table 4.3. IC_{50} and MIC values of growth inhibition assays of PGG against 24 *A. baumannii* strains. These values represent the concentration (μg/mL) of extract or antibiotic needed to inhibit 50% and 90% of bacterial growth, relative to the vehicle (DMSO) control. "-" indicates that the value was not detected at the tested concentrations of 2-256 μg/mL for PGG, 2-16 μg/mL for meropenem (Mem), and 0.5-4 μg/mL for colistin (Cst), indicating that the value is above the tested concentrations.

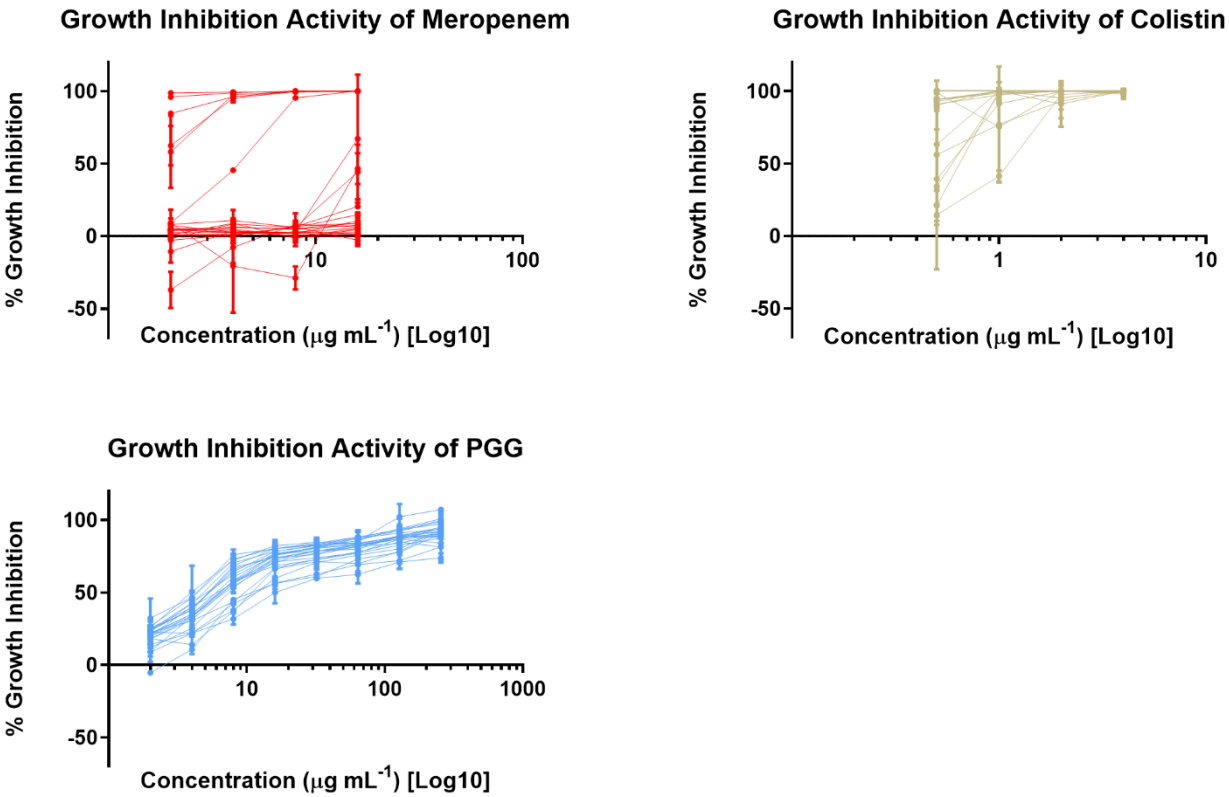

Figure 4.4. Growth inhibition curves for PGG tested against twenty-four *A. baumannii* strains. Each curve represents a different bacterial strain. Data represent percent growth inhibition relative to the vehicle (DMSO) control.

Biofilm inhibition and eradication assays against *A. baumannii*

Biofilm formation inhibition and biofilm eradication assays were performed to assess for the activity of PGG against *A. baumannii* AB5075. Figure 4.5 shows the results of both assays, as compared to the false positive control tetracycline. Tetracycline is an antibiotic for which AB5075 remains susceptible (Jacobs et al., 2014), but no positive control is known for the formation inhibition or eradication of biofilm in AB5075. Thus, the starting concentration of tetracycline for

the formation inhibition assay was 64 µg/mL and showed inhibition of bacterial growth while the starting concentration of PGG extract was subIC$_{50}$ (4 µg/mL) in order prevent complete bacterial growth inhibition. Because the purpose of the eradication assay was to assess for the eradication of biofilm after biofilm had already grown, the starting concentration of PGG in the eradication assay did not need to be subIC$_{50}$. The results show that PGG does not inhibit AB5075 biofilm formation or eradicate biofilm once it has already formed.

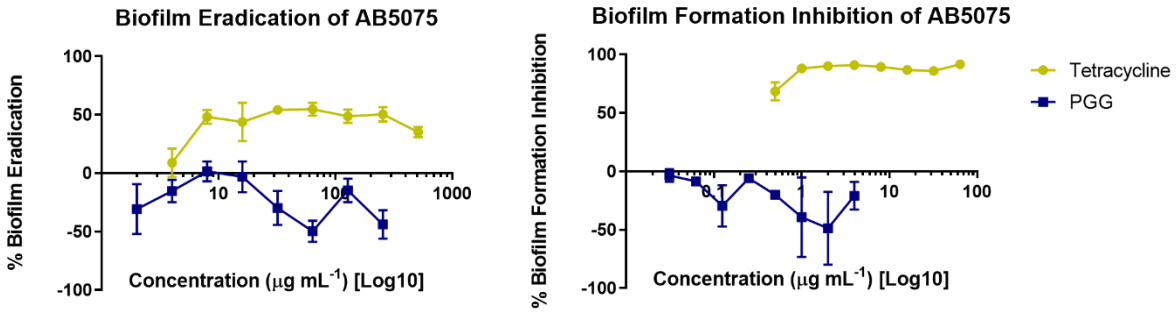

Figure 4.5. Biofilm formation inhibition and eradication of *A. baumannii* AB5075 by PGG. For formation inhibition, the starting concentration of PGG was the subIC$_{50}$ while the starting concentration of tetracycline was the MIC. For eradication, extract and antibiotic control (tetracycline) were tested at growth inhibitory concentrations. The percent formation inhibition and percent eradication values were calculated relative to the vehicle control (DMSO).

Supplementation assays

Growth inhibition activity of PGG in supplemented and iron-depleted media

To quantify the effect of iron and lipid supplementation on PGG's inhibitory activity against *A. baumannii*, growth inhibition assays were performed of PGG against AB5075 with addition of iron or lipid to the media. For iron studies, one assay utilized iron (II) sulfate ($FeSO_4$) in the medium while the other assay was performed with iron (III) sulfate hydrate ($Fe_2(SO_4)_3 \cdot H_2O$) supplementation. For lipid studies, assays involving 0.02% oleic acid and 0.02% polysorbate 80 supplementation were performed. For the iron-depletion assay, the CAMHB utilized for the

overnight and working cultures was first treated with Chelex resin, which binds and removes metal ions including iron. Figure 4.6 shows the growth inhibition curves of these assays, with meropenem as the antibiotic control for which supplementation does not affect, and Table 4.4 compares the IC_{50} values of PGG in each condition. The assays show that PGG's inhibitory activity for AB5075 is severely attenuated by the addition of both iron (II) and iron (III) to the media. On the other hand, oleic acid supplementation did not result in decrease in inhibition while polysorbate 80 supplementation caused PGG's IC_{50} to increase.

		IC_{50} (μg/mL)	
Media	Supplement	PGG	Meropenem
CAMHB	Control	8	32
	Oleic acid	8	32
	Polysorbate 80	128	32
	Iron (II) sulfate	>256	32
	Iron (III) sulfate	>256	32
	Iron-depleted	8	32
TSB	Control	32	32-64

Table 4.4. IC_{50} values of growth inhibition assays of PGG against *A. baumannii* AB5075 in supplemented media and iron-depleted media. These values represent the concentration (μg/mL) of extract or antibiotic needed to inhibit 50% of bacterial growth, relative to the vehicle (DMSO) control.

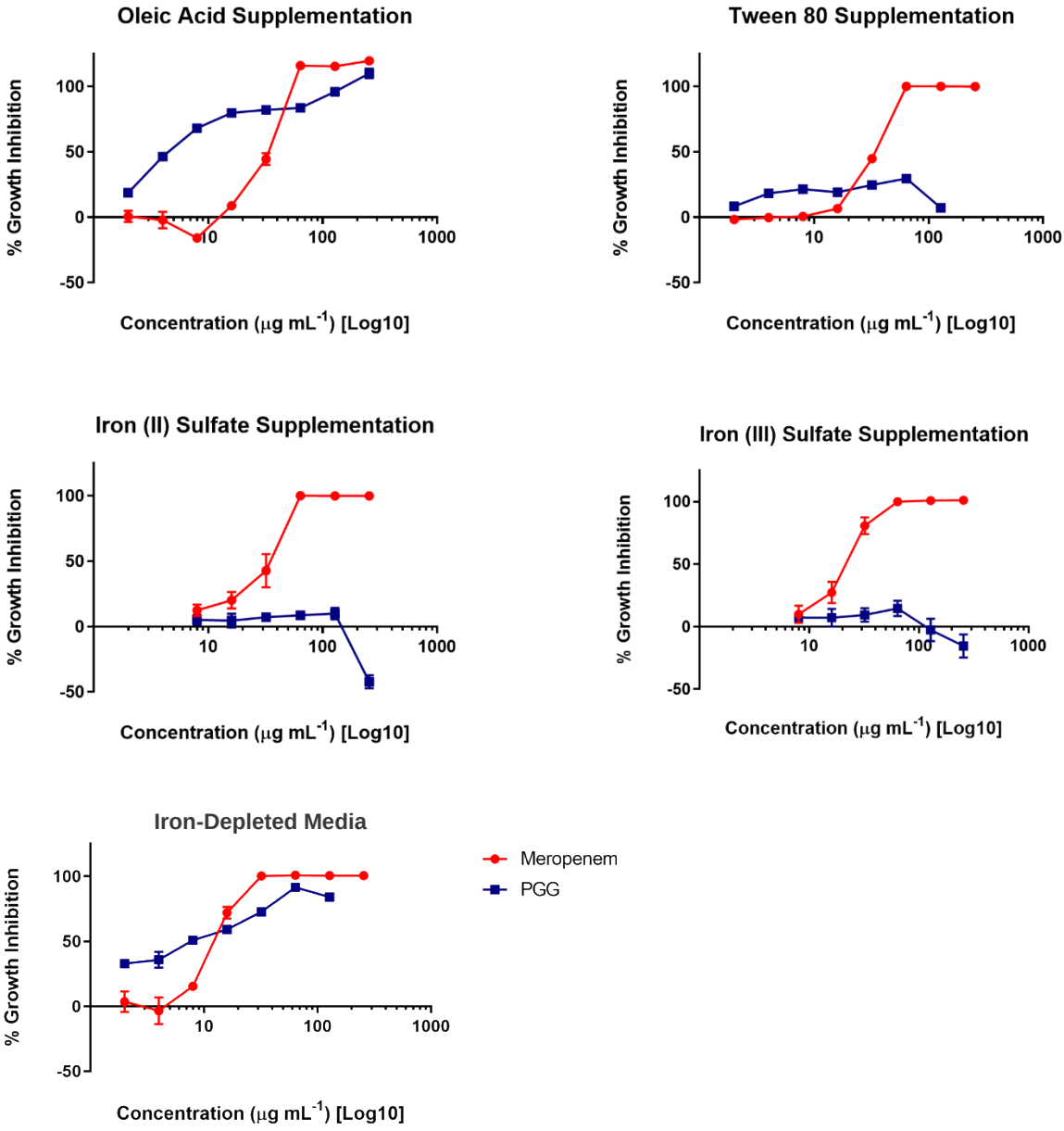

Figure 4.6. Growth inhibition assays of PGG against *A. baumannii* AB5075 with supplementation of media with iron (II), iron (III), oleic acid, and polysorbate 80, and in iron-depleted media. Data represent percent growth inhibition relative to the vehicle (DMSO) control.

Optical density quantification of PGG supplemented with iron

After noting that addition of iron to media containing PGG affects the color of the media, I performed an optical density assay of decreasing concentrations of PGG, supplemented with 1

mM of iron (II) sulfate ($FeSO_4$) and iron (III) sulfate ($Fe_2(SO_4)_3 \cdot H_2O$). Figure 4.7 shows the color difference between PGG alone and PGG supplemented with iron in the 96-well plates.

Figure 4.8 quantifies these differences in optical densities. The color of PGG mixed with iron became a dark lilac purple, and the optical densities (600 nm) of the mixtures of PGG and iron were higher than those of PGG in media alone. As the concentration of PGG was decreased, the mixture lightened, and the optical densities decreased as well. Of particular note is the higher optical densities of PGG mixed with iron (III) sulfate hydrate, as compared to the optical densities of PGG mixed with iron (II) sulfate.

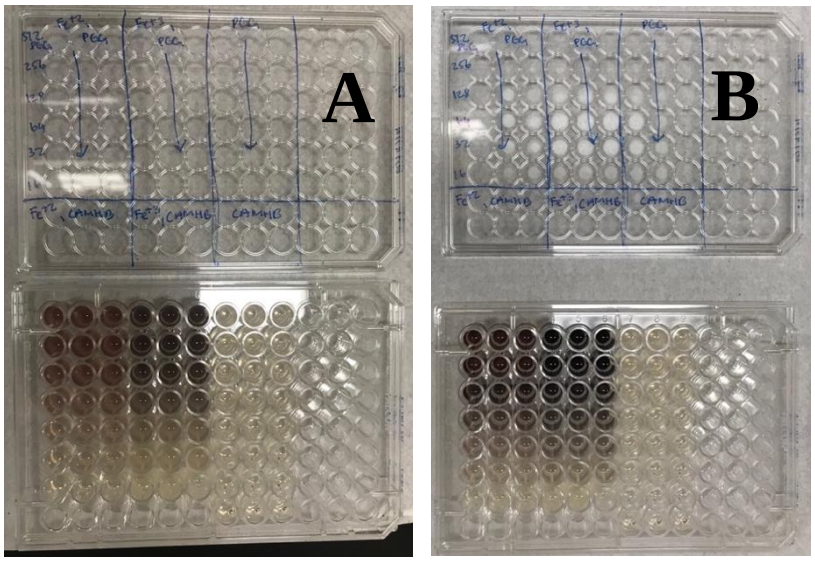

Figure 4.7. Optical density assay plates at (A) 0 hours and (B) 24 hours after plating. The plate was incubated statically at 35 °C during the 24-hour period.

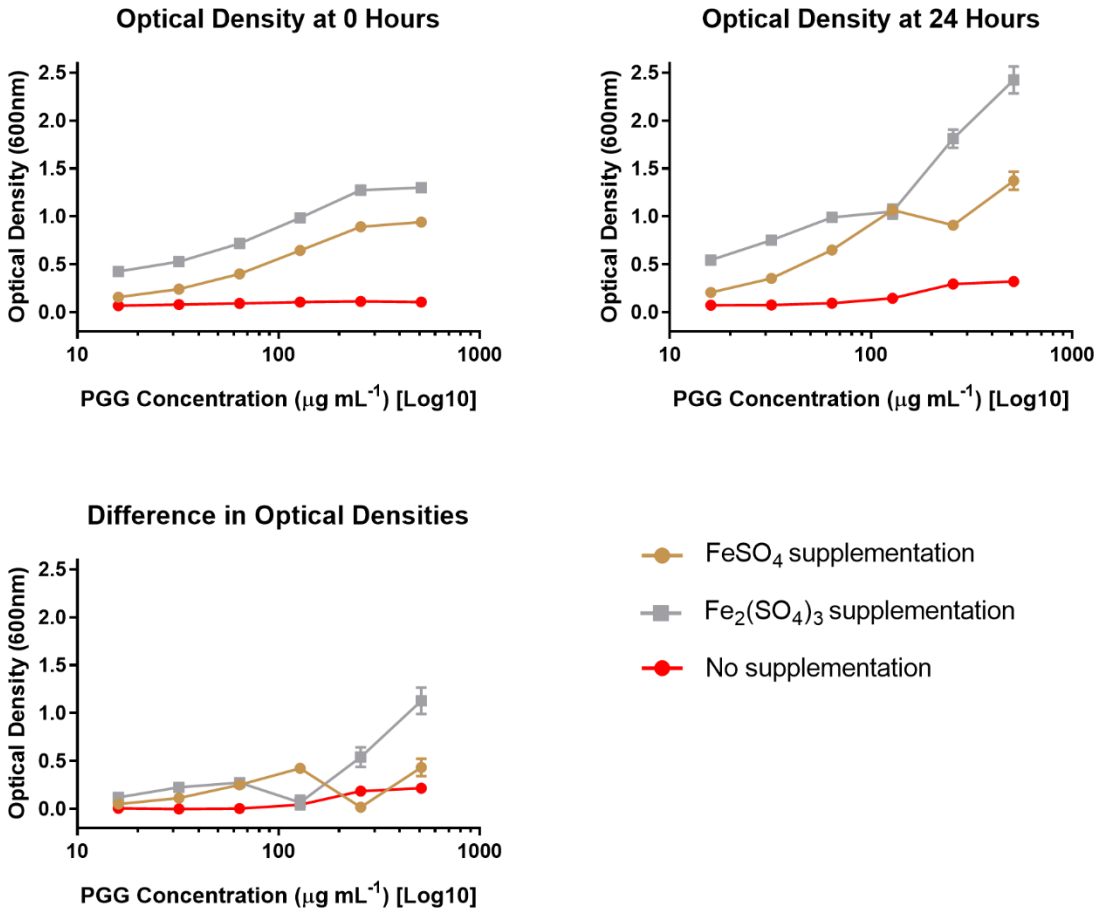

Figure 4.8. Optical density readings of solutions of PGG supplemented with 1 mM of iron (II) sulfate and iron (III) sulfate. Iron (II) sulfate and iron (III) sulfate were added to decreasing concentrations of PGG in CAMHB. The optical density readings were measured at 600 nm.

Time-kill assays

Time-kill assays were performed to quantify the number of colony-forming units per mL (CFU/mL) of *A. baumannii* AB5075 that arise in the presence of treatment at different time points. PGG was tested at a concentration of 256 µg/mL (MIC of PGG against AB5075), while meropenem, the antibiotic control, was tested at 64 µg/mL (MIC of meropenem against AB5075). To compare the effects of normal PGG treatment with that of media supplementation, time-kill assays were also performed in the presence of 1 mM iron (II) sulfate, 0.02% oleic acid, and 0.02%

polysorbate 80. Figure 4.9 shows the CFU/mL of bacterial growth at different time points. At the 24-hour timepoint, the CFU/mL measurements of oleic acid, polysorbate 80, and iron (II) sulfate supplementation conditions were approximately 10-fold, 100-fold, and 1000-fold higher than the CFU/mL measurement of PGG alone.

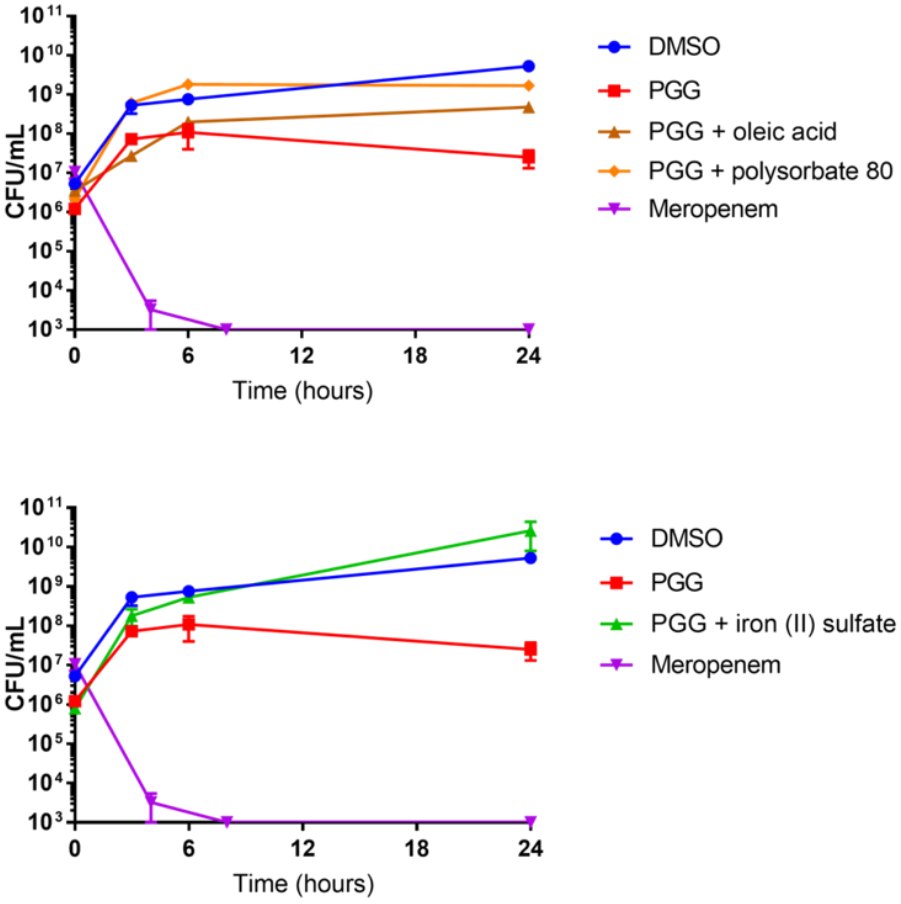

Figure 4.9. Time-kill assays of PGG against *A. baumannii* AB5075 alone, with lipid supplementation, and with iron (II) sulfate supplementation. PGG was tested at a concentration of 256 µg/mL while meropenem was tested at 64 µg/mL. The curves denote the number of colony-forming units per mL at various timepoints.

Resistance studies

Spontaneous mutant assays

Spontaneous mutant assays were performed to assess the propensity of *A. baumannii* AB5075 to develop resistance against PGG, and to test if iron supplementation would restore bacterial growth. Figure 4.10 and Figure 4.11 show the results of the assays performed on Petri plates and 96-well plates, respectively. For the Petri plate assay, 24 hours of incubation resulted in a full lawn of growth on the control plate and no visible bacterial growth on PGG-treated plates (Day 1: pre-iron supplementation, Figure 4.10). For the 96-well assays, after 24-hours, there was bacterial growth in all of the control wells and in a single 0.5 x MIC treatment well, but no growth was evident in any of the other 0.5 x MIC, 1 x MIC, and 2 x MIC wells (Figure 4.11). For the second half of the assay, 1 mM of iron (II) sulfate was spread across the 0.5 x MIC and 2 x MIC Petri plates; the 96-well assay had supplementation conditions for both 1 mM of iron (II) sulfate and 1 mM of iron (III) sulfate for all of the PGG-treated wells. After addition of iron to the agar, all wells containing PGG became a purple color, increasing in darkness with increasing PGG concentration. The wells with PGG and iron also increased in darkness over time. After 24 hours of incubation, the 0.5 x MIC Petri plate exhibited a full lawn of growth, while the 2 x MIC plate and the non-iron-supplemented 1 x MIC plate remained free of visible colonies. For the 96-well assays, colonies were visible in all of the 0.5 x MIC wells, except a single iron (III) supplemented, 0.5 x MIC well in TSA. Another 48 hours of incubation resulted in darker media and exemplified growth in all of the wells with restored growth.

Day 1: pre-iron supplementation

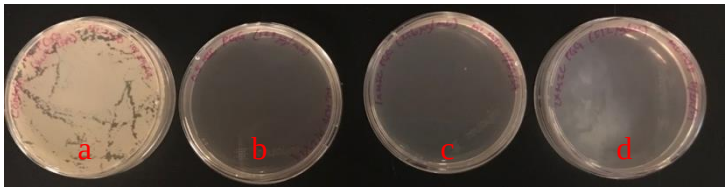

Day 2: with iron supplementation

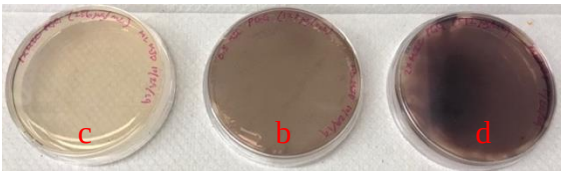

Figure 4.10. Growth of AB5075 on TSA plates with PGG treatment, followed by iron (II) supplementation. The Day 1 picture was taken after twenty-four hours of incubation at 35 °C, prior to iron (II) supplementation. Iron (II) sulfate was subsequently spread onto the 0.5 x MIC and 2 x MIC plates. The Day 2 picture was taken after twenty-four hours of incubation at 35 °C of the iron supplemented plates. Labels a, b, c, and d represent the control (no PGG added), 0.5 x MIC of PGG, 1 x MIC of PGG, and 2 x MIC of PGG plates, respectively.

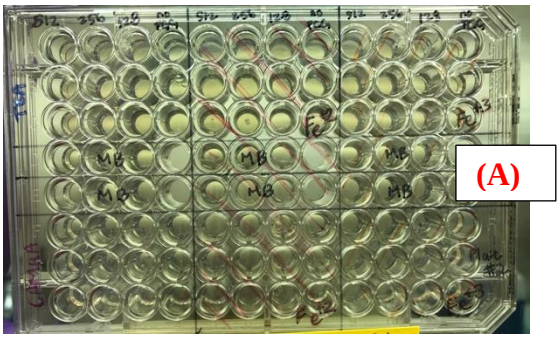

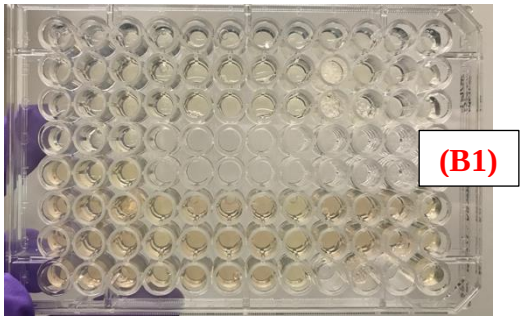

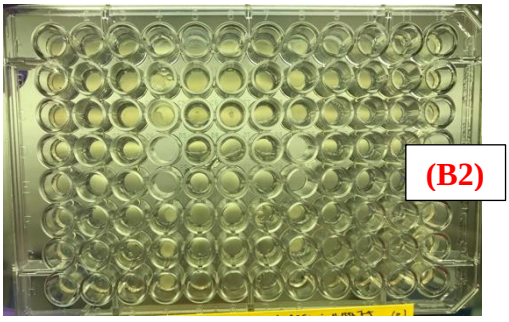

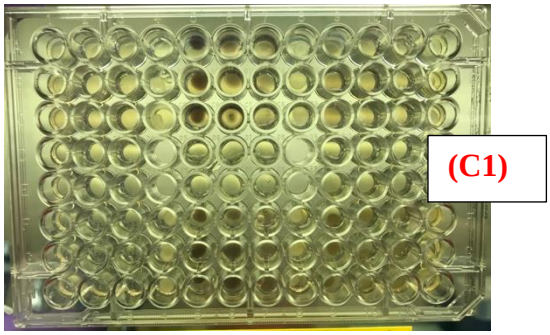

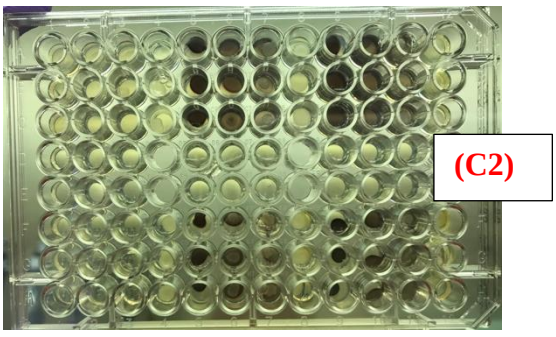

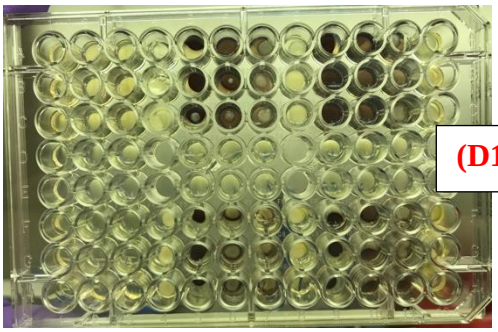

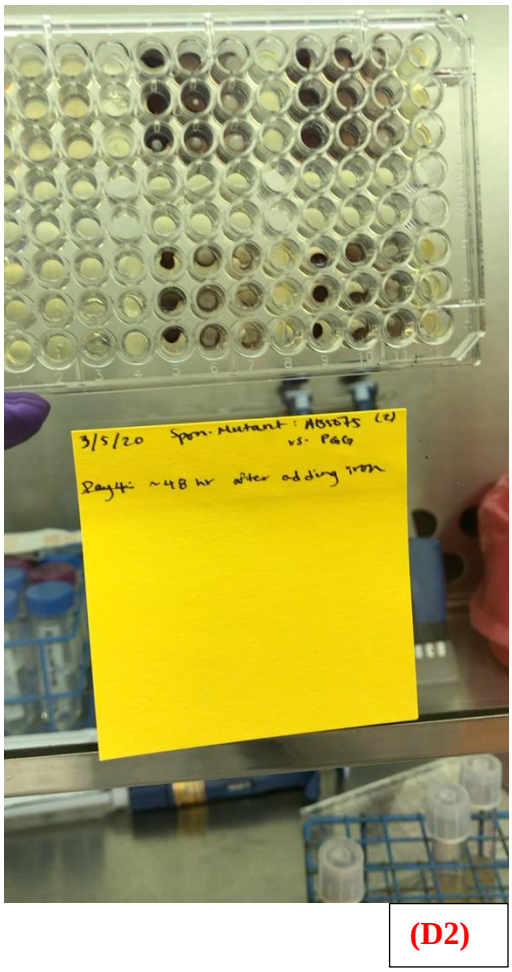

Figure 4.11. Growth of AB5075 on a 96-well plate with PGG treatment, followed by iron (II) and iron (III) supplementation. (A) represents the plate layout: TSA and CAMHA wells were treated with 0.5 x MIC, 1 x MIC, and 2 x MIC, and then supplemented with iron (II) sulfate and iron (III) sulfate following 24-hours of incubation at 35 °C. Media blank wells (MB) received neither PGG treatment, nor iron supplementation. (B1) and (B2) represent 0 and 24 hours after addition of bacterial culture, prior to iron supplementation. (C1) and (C2) represent 0 and 24 hours after adding iron. (D1) and (D2) represent 48 hours after adding iron, in image and video form, respectively.

Serial resistance passaging

To test the evolution of resistance, a 21-day serial passaging experiment of *A. baumannii* AB5075 was performed in the presence of PGG and tetracycline, which had starting MICs of 256 µg/mL and 4 µg/mL, respectively, for day 1. Each serial passage involved using culture from the previous day's 0.5 x MIC wells and treating with PGG and tetracycline in a gradient. Over the three-week serial passaging experiment, PGG maintained a stable MIC while the MIC of tetracycline increased by 16-fold, increasing from 4 µg/mL (susceptible) to 64 µg/mL (resistant). Any day-to-day increase from the initial MIC of PGG fluctuated back down to the initial MIC of 256 µg/mL shortly after.

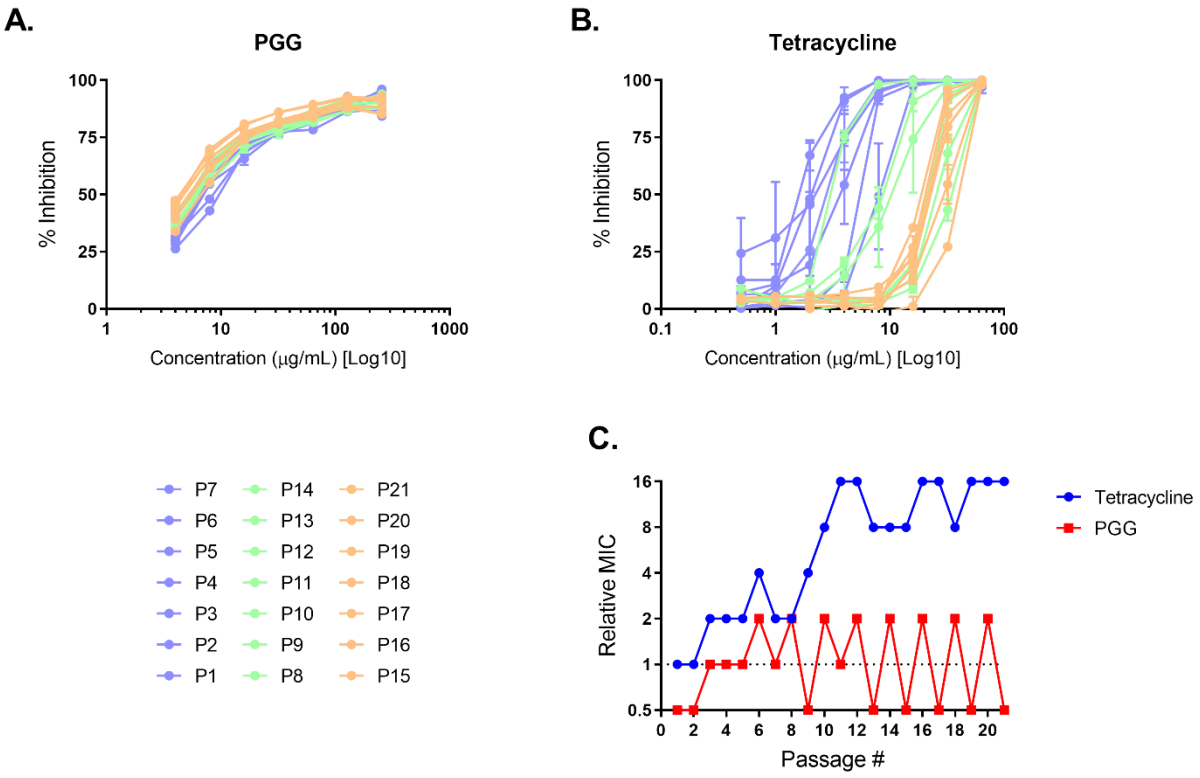

Figure 4.12. Resistance serial passaging of *A. baumannii* AB5075 in the presence of PGG and tetracycline. Passages were repeated daily, for 21 days. The curves in (A) and (B) represent percent growth inhibition calculated relative to the vehicle (DMSO) control for each day; the legend shows the daily passages. (C) shows the relative MIC values for each passage.

Cytotoxicity assays

Cytotoxicity assays were performed on immortalized human keratinocytes (HaCaTs) using a lactate dehydrogenase (LDH) experiment. PGG has an IC_{50} of 256 μg/mL for the assay. At the median IC_{50} of PGG against *A. baumannii*, this corresponds to a therapeutic index of 32.

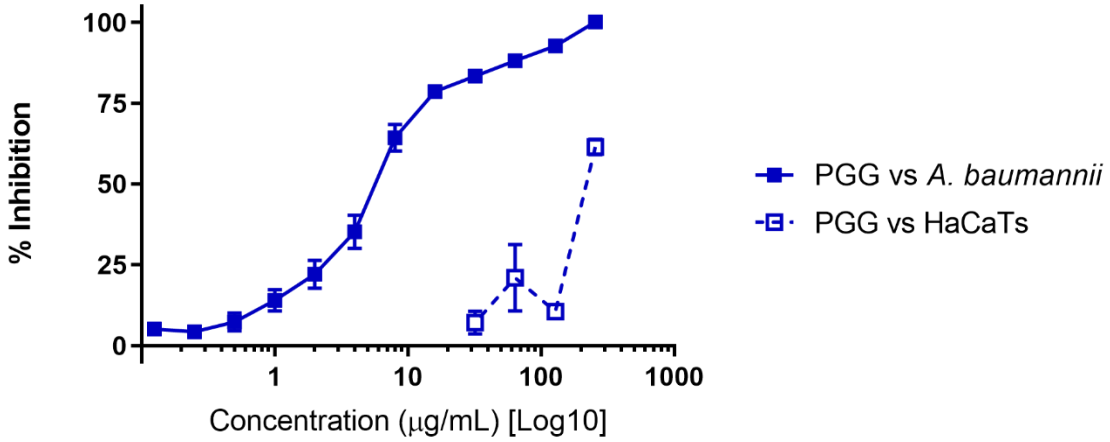

Figure 4.13. Growth inhibition of *A. baumannii* CDC35 and HaCaT cytotoxicity by PGG.

Compound confirmation

Preliminary co-injection study

A preliminary co-injection study was performed for analysis of PGG in 1271C. The chromatograms of PGG by itself and of PGG + 1271C co-injection reveal a common peak (around 10 minutes) that suggests presence of PGG in 1271C (Figure 4.14). The UV spectra of this suspected PGG peak is the same for the PGG standard and 1271C, further verifying presence of PGG in 1271C (Figure 4.15). Table 4.5 shows that the area of the suspected PGG peak increased, from 1271C alone to co-injection of 1271C + PGG. Figure 4.16 shows the chemical structure, formula, and molar mass of PGG.

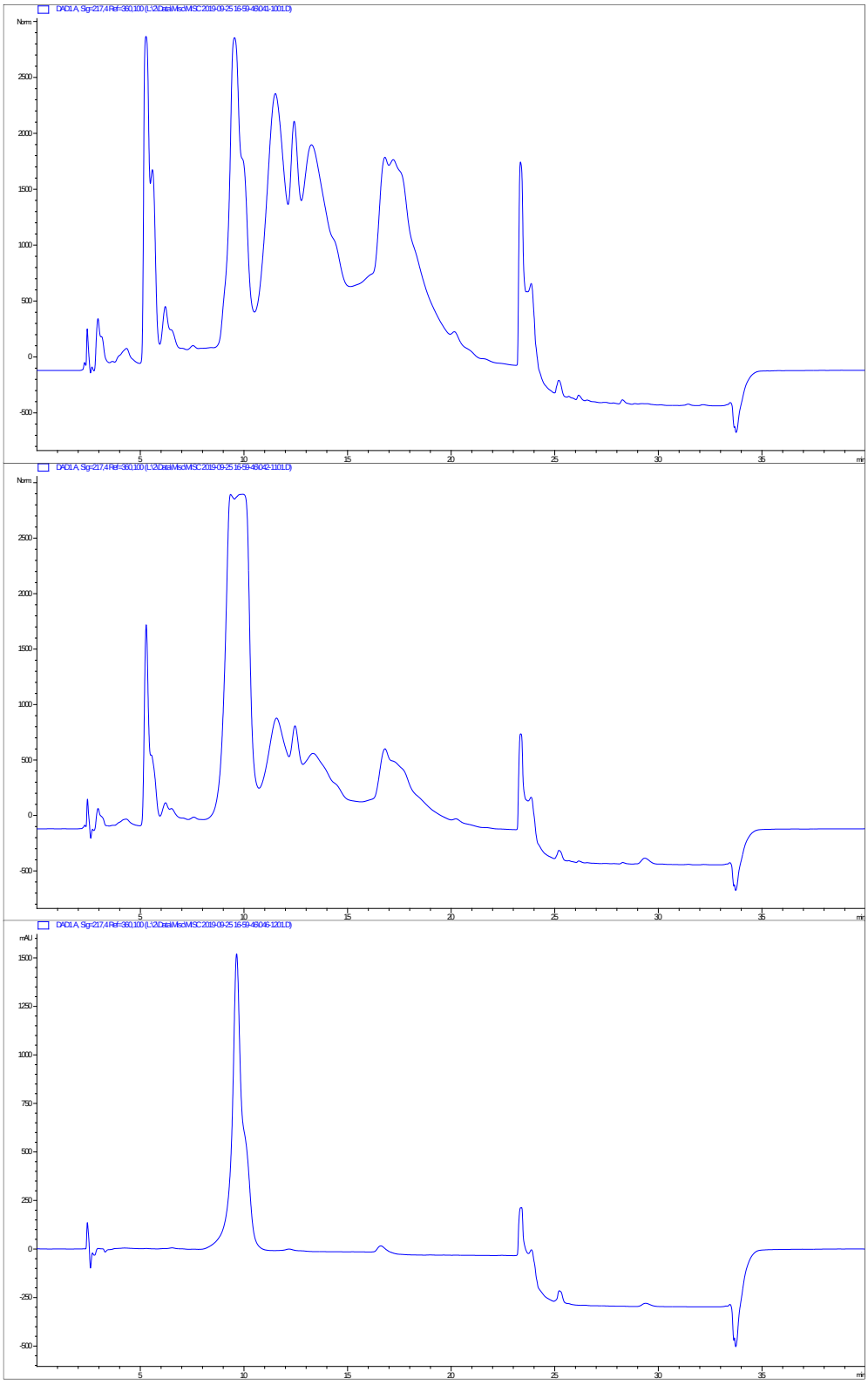

A. 1271C

B. 1271C + PGG co-injection

C. PGG standard

Figure 4.14. Chromatograms of co-injection of 1271C + PGG at 217 nm. Co-injection of 1271C and PGG (B) reveals a peak found also in the injection of pure PGG standard (C) at approximately 9.5 to 10 minutes.

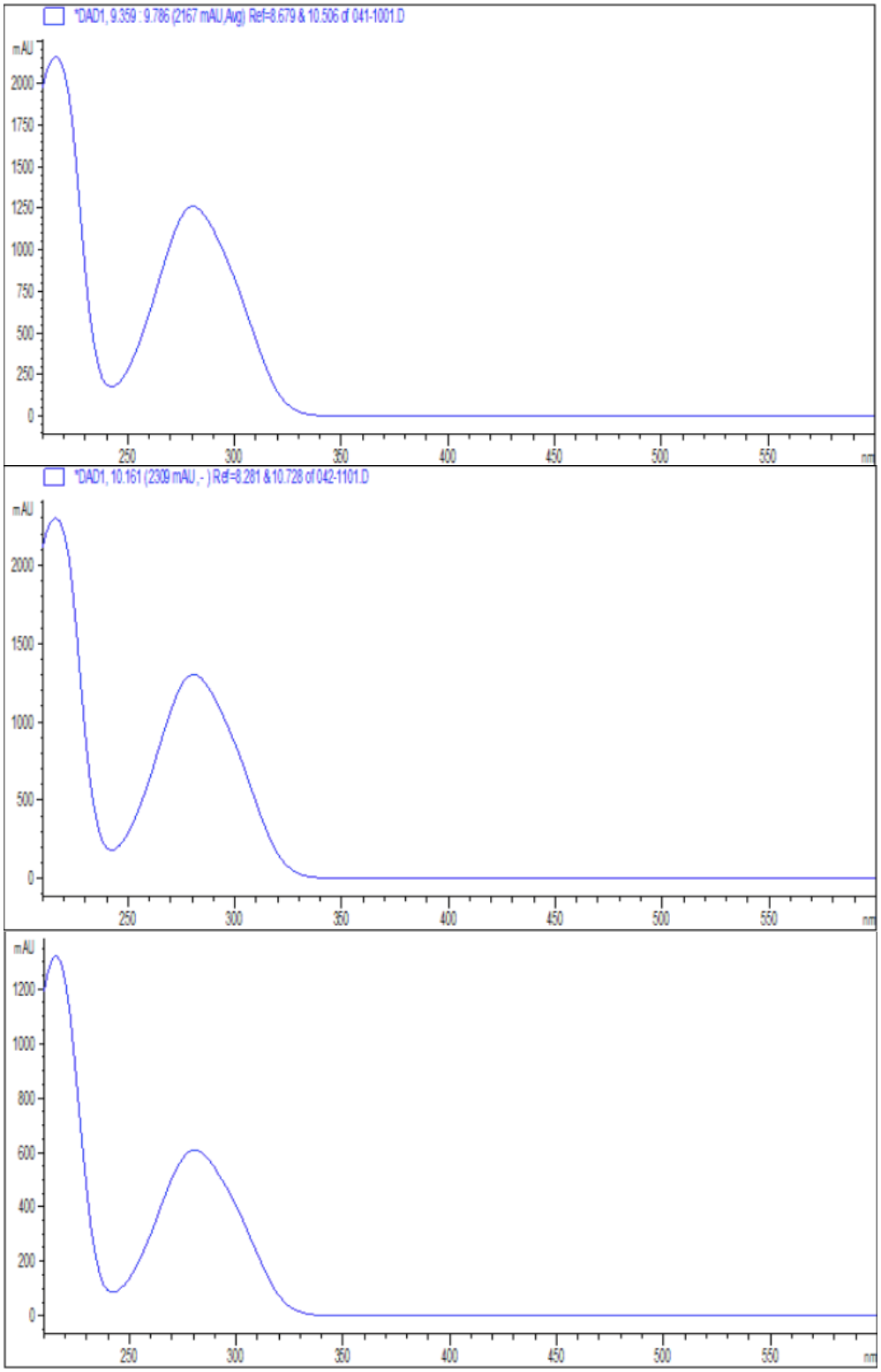

A. 1271C

B. 1271C + PGG co-injection

C. PGG standard

Figure 4.15. UV spectra of the suspected PGG peak in 1271C, co-injection of 1271C + PGG, and PGG standard. The suspected PGG peak appeared at approximately 9.5 to 10 minutes.

	Peak Area	Peak Height	Time of Peak (min)
Rhus coriaria (1271C)	103,542.3	2,358.4	9.54
1271C + PGG co-injection	113,453.7	7,420.9	10
PGG	57,114.7	1,525.8	9.48

Table 4.5. Area, height, and time of suspected PGG peak in 1271C, co-injection of 1271C + PGG, and PGG standard.

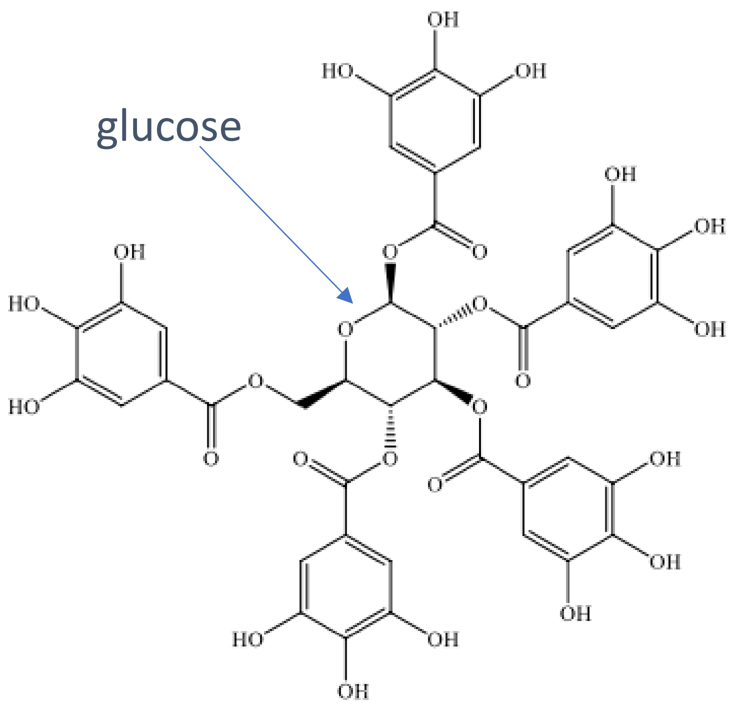

Figure 4.16. Chemical structure of pentagalloyl glucose (PGG). PGG is composed of a central glucose and five galloyl groups. The chemical formula is $C_{41}H_{32}O_{26}$, and the molar mass is 940.7 g/mol.

CHAPTER 5: DISCUSSION

Previous studies of the hydrolysable gallotannin pentagalloyl glucose (PGG) demonstrate the compound's significant antioxidant, anti-cancer, anti-viral, anti-microbial, anti-inflammatory, and anti-diabetic activity (Torres-León et al., 2017). PGG is well researched for its growth inhibition and biofilm inhibition activity of particular Gram-positive bacteria, like *Staphylococcus aureus* (Lin, Chang, Hua, Wu, & Liu, 2011) (Lin, Shu, Huang, & Cheng, 2012), but a paucity of research on its activity against Gram-negative bacteria such as *Acinetobacter baumannii* motivated further investigation of PGG. A microbiological characterization of its efficacy against selected bacterial strains presents PGG as a potential bacteriostatic topical treatment against even highly resistant *A. baumannii*. Its growth inhibition activity may be attributed to iron chelation and/or lipid interaction. Resistance passaging experiments suggest that resistance to the compound does not develop quickly.

PGG in natural products

Early investigations involved an extract isolated from the plant *Rhus coriaria*, which was previously found to be active against *A. baumannii* in preliminary screens of the Quave Natural Product Library (QNPL). To begin study of the extract (extract 1271), I explored both traditional and modern scientific libraries for information on the sumac plant, and then conducted bio-guided fractionation of 1271 through liquid-liquid partitioning and growth inhibition assays. Early results presented extract 1271C, the ethyl acetate partition of the sample, as the partition with the highest growth inhibition activity - and thus the partition that I would continue fractionating and performing microbiological assays. Concurrent research performed on *Schinus terebinthifolia,* another prolific member of the QNPL's Anacardiaceae collection, found PGG to be its active compound. With this and previous literature documenting the presence of PGG in other *Rhus*

species (Cho, Sohn, Lee, & Kim, 2010) (Ma et al., 2012), I predicted PGG to be an active constituent of 1271C. While the remaining majority of **Chapter 5: Discussion** concentrates on the microbiological effect of PGG on *A. baumannii* and its possible mechanisms of action, earlier assays involving 1271C also provide valuable insight to *R. coriaria*'s functionality as a traditional medicine.

Using chemical polarity data surmised from flash chromatography and analytical HPLC runs, I modified our lab's analytical HPLC sequence for PGG to perform co-injection studies of the commercial compound against 1271C. The co-injection studies indicated PGG to be a component of 1271C through two pieces of evidence. Firstly, injecting both commercial PGG and 1271C solutions into the same HPLC column revealed a common peak in the resulting chromatograms. This common peak is likely the representation of PGG, indicating that PGG is indeed a component of 1271C (Figure 4.14). Secondly, the UV spectra of the suspected PGG peak revealed the same peaks in the 1271C and pure PGG samples (Figure 4.15). The area of the suspected PGG peak in the co-injection run (1271C + PGG) was larger than the areas of the peak in the PGG alone run and 1271C alone run (Table 4.5). Further directions involve fractionating 1271C to a greater extent, modifying the HPLC sequence to better separate the extract, and re-running the co-injection experiment to achieve more separated peaks and confirm PGG existence.

Liquid-liquid partitioning revealed that the large majority (65.54%) of the ethanoic extraction of *R. coriaria* leaves is in the ethyl acetate partition, which is also the partition with the highest growth inhibition activity. This indicates that the majority of soluble phytochemicals, and likely the majority of active compounds, in 1271 share a polarity most similar to ethyl acetate, a polar solvent with a single carbonyl group. When compared to other active extracts of the QNPL, these results appeared similar to those of extract 1722, isolated from *Rhus copallinum* leaves,

whose preliminary *A. baumannii* screens also showed the ethyl acetate partition (1722C) to be the most active.

Given the co-injection results and the fact that *R. coriaria*, *R. copallinum*, and *S. terebinthifolia* share a common family origin (Anacardiaceae), PGG is a putative active constituent in 1271C and 1722C. In growth inhibition assays of pure PGG, 1271C, and 1722C against the "ESKAPE" panel pathogens, the growth inhibition curves for the three extract treatments were similar for the selected bacterial strains, except for *Enterococcus faecium* EU-44 (which showed similar curves for PGG and 1271C but not for 1722C). The discrepancy of results for EU-44 may be explained by each extract's unique chemical profiles. For each bacterial strain, PGG had the highest percent growth inhibition at each concentration, followed by 1271C and then 1722C. An interpretation of the results is that 1271C and 1722C contain a mixture of many other active and non-active compounds besides PGG. A full bio-guided fractionation process would reveal if there are other compounds of interest and confirm that PGG is an active compound in these extracts. A mass spectrometry measure of the extracts would also definitively confirm PGG's presence.

PGG, as discussed in the remainder of this chapter, presents as a valuable tool against MDR *A. baumannii*. The chemical isolation of this compound from natural products is worthy of further exploration.

PGG: a promising topical agent for growth inhibition of *A. baumannii*

To characterize the effect of PGG against a broad range of resistant and increasingly resistant bacterial species, growth inhibition assays were performed in broth microdilution. To my knowledge, this study is the first to identify the MIC and IC_{50} values of PGG for both ESKAPE pathogens and a selected panel of *A. baumannii* strains, in order to further guide the compound's development as a drug. The compound maintains varied MIC and IC_{50} values across each of the

six strains of ESKAPE pathogens, with notably low MIC and IC_{50} values for *P. aeruginosa* (16 μg/mL and 4 μg/mL, respectively), *S. aureus* (64 μg/mL and 16 μg/mL, respectively), *A. baumannii* (64 to 256 μg/mL and 8 to 64 μg/mL, respectively), and *E. faecium* (64 μg/mL and 32 μg/mL, respectively). The MIC and IC_{50} values were relatively higher for *E. cloacae* (>256 μg/mL and 32 μg/mL, respectively) and *K. pneumoniae* (>256 μg/mL and 16 μg/mL, respectively).

The ESKAPE assay results indicate that PGG is a broad-spectrum agent that has inhibitory effects on both Gram-negative and Gram-positive bacteria, corroborating previous reporting of PGG's broad-spectrum activity (Cho et al., 2010). This suggests that PGG's mechanism of action targets a bacterial feature or environmental necessity that is common to multiple bacterial species, regardless of their membrane or resistance profile groupings. As with other broad-spectrum agents, PGG has potential as an empirical medicine for infections in which the causative agents are not immediately known. The positive correlation of empirical antibiotic therapy failure and bacterial resistance is a well-documented phenomenon, particularly in cases of inappropriate antibiotic use (Merli et al., 2015). The inappropriate use of empirical antibiotic therapy may prove not only ineffective against critical clinical infections, but it may also be a driver of multidrug resistance. Thus, effective and improved therapy involves discriminating for appropriate use, as well as investigating possible empirical agents like PGG that do not induce resistance rapidly (discussed later in this section). In addition, the broad-spectrum status of PGG introduces prospects of usage for superinfections, in which the affected patient has contracted multiple bacterial infections that each respond to different antibiotics. Although this Thesis does not delve further into the multi-bacteria prospects of the compound or the mechanisms against each bacterial species, these questions may be pursued in the future.

Growth inhibition assay results also show that PGG has generally consistent inhibitory activity against *A. baumannii* strains with differing resistance profiles, with MIC and IC_{50} values that range from 64 to >256 μg/mL and 8 to 64 μg/mL, respectively. Of the twenty-four total *A. baumannii* strains tested, seven strains had MIC values greater than 256 μg/mL. However, the growth inhibition of these strains at 256 μg/mL were close to the 90% growth inhibition threshold (Table 4.3), and future reproductions of the assay may result in MIC values of 256 μg/mL. To compare PGG and antibiotic activity against resistant strains, the antibiotics meropenem and colistin were included in the same assays. The MIC and IC_{50} values for colistin, a last-resort antibiotic used for Gram-negative bacteria, ranged from <0.5 to 4 μg/mL and 1 μg/mL, respectively. The MIC and IC_{50} values for meropenem, a broad-spectrum antibiotic with conferred resistance for many strains, ranged from <2 to >16 μg/mL and >16 μg/mL, respectively. These results further validate PGG's use against a wide range of resistant *A. baumannii* - many of which are resistant to common antibiotics.

Particular attention was focused on testing the efficacy of PGG against resistant *A. baumannii*. Thus, for several characterization assays, the multidrug resistant (MDR) strain AB5075, was the pathogenic model of choice due to its known resistance to a wide panel of antibiotics: amikacin, ampicillin, cefepime, ceftazidime, ciprofloxacin, gentamicin, imipenem, meropenem, and tobramycin (Jacobs et al., 2014). A time-kill analysis was performed to determine the number of colony-forming units per mL at various time-points during *A. baumannii* AB5075 growth. At the MIC concentration of 256 μg/mL, PGG was determined to be a bacteriostatic agent against AB5075. The distinction between bacteriostatic and bactericidal lies in how the antimicrobial inhibits bacterial growth - with the former simply inhibiting bacterial growth without completely killing cells, and the latter killing the cells. Although this distinction might lead to an

intuitive deduction that bactericidal agents are superior to bacteriostatic agents, clinical reviews suggest that bactericidal agents are not generally superior for infection treatment, and therapeutic decisions should instead be made on other quantified data (Wald-Dickler, Holtom, & Spellberg, 2018) (Nemeth, Oesch, & Kuster, 2015). In some cases, bacteriostatic agents are actually advantageous because they reduce the production of toxins by bacteria (Pankey & Sabath, 2004). In addition, PGG's status as a bacteriostatic agent provides clues to its mechanism for future investigators; in some way or another, PGG inhibits AB5075 cell growth by keeping cells in the stationary growth phase, rather than by completely killing them.

The same MDR strain AB5075 was used to test for the propensity to develop resistance. In the spontaneous mutant assays performed on TSA Petri plates and on 96-well plates, AB5075 was spread on agar containing PGG at 0.5 x MIC, 1 x MIC, and 2 x MIC (128, 256, and 512 µg/mL, respectively) and incubated for 24 hours to allow any spontaneous mutants to grow. Colonies grew throughout the control plate without PGG treatment, and the 1 x MIC and 2 x MIC treatment plates did not exhibit growth. For the 0.5 x MIC treatment condition, a single well in a single 96-well assay exhibited bacterial growth, which may be attributed to the fact that this well was under the MIC for AB5075, or to the possibility that PGG was not as evenly distributed in the area that bacterial working culture was added. In totality, these results suggest that spontaneous mutants that would be resistant to PGG did not develop, but numerous trials of this assay must be performed before any conclusions can be drawn about the rarity of spontaneous resistant mutants. To test for the evolution of resistance, AB5075 was subjected to a three-week serial passaging experiment, in which bacteria growing in the presence of 0.5 x MIC of PGG were transferred to a fresh plate of media and PGG each day. Results show that PGG maintained a stable MIC throughout the twenty-one-day experiment, indicating that the MDR strain AB5075 did not evolve

resistance to the compound. Any daily increase from the initial MIC of PGG fluctuated back down to the initial MIC of 256 µg/mL soon after. Such promising results appear even more relevant when compared to the evolution of resistance of the same strain to tetracycline, the antibiotic control. The MIC of tetracycline, a broad-spectrum and bacteriostatic agent as well, increased from 4 µg/mL (susceptible) to 64 µg/mL (resistant). This 16-fold increase in MIC occurred after only 10 passages, which is consistent with what current literature suggests of AB5075's high propensity for antibiotic resistance (Jacobs et al., 2014). It is possible that the mechanism that PGG acts through is not one that is particularly vulnerable to resistance development; thus, the AB5075 did not evolve resistance to the compound while surpassing the resistance breakpoint for tetracycline. Because the bacterial cultures from the day 12 and 21 passages were cryopreserved, follow-up experiments to this Thesis may involve characterizing the preserved samples.

This Thesis is the first - to my knowledge - to document PGG's inhibitory activity against *A. baumannii* and validate the traditional use of *R. coriaria*. This study also validates the traditional use of *S. terebinthifolia* and *R. copallinum*, as supported by previous literature (Cho et al., 2010; Muhs et al., 2017). The promising portrait of PGG as a bacteriostatic agent with relatively low vulnerability to resistance paints a therapeutic future. Cytotoxicity assays with human keratinocytes (HaCaTs) were performed to evaluate the in vivo utilization of the compound. Results yielded an IC_{50} of 256 µg/mL for mammalian cells and a therapeutic index of 32 for PGG's growth inhibition of *A. baumannii*, suggesting that the compound may be an effective topical treatment.

Iron chelation as a possible mechanism of action

Previous mechanistic studies suggest that PGG is an iron chelator that inhibits *S. aureus* biofilm formation (Lin et al., 2011) (Lin et al., 2012). In biofilm experiments on polystyrene and

polycarbonate surfaces, Lin et al. showed that PGG decreases *S. aureus* SA113 biofilm formation by sequestering iron, an important mineral for both the initial attachment to solid surfaces and the production of polysaccharide intercellular adhesin. In order to examine PGG's mechanism of inhibiting *A. baumannii* growth, I performed iron supplementation studies that were conceptually similar to those performed by Lin et al.

To begin, growth inhibition assays of *A. baumannii* AB5075 were performed in CAMHB supplemented with 1 mM of iron. For both types of iron supplementation (iron (II) sulfate and iron (III) sulfate), growth inhibition was attenuated. Compared to the growth inhibition activity of PGG against AB5075 in regular CAMHB, the IC_{50} value with iron supplementation increased more than 32-fold, from 8 µg/mL to >256 µg/mL. Time-kill assays of PGG against AB5075 revealed a 1000-fold increase in colony-forming units per mL for iron (II) supplemented condition, compared to assays with PGG alone. When the same growth inhibition assays were repeated in iron-depleted CAMHB, the growth inhibition activity of PGG was higher than in both iron supplementation and regular CAMHB conditions. Compared to the MIC for PGG in regular CAMHB, there appeared a 4-fold decrease in MIC for PGG in iron-depleted CAMHB, from 256 µg/mL to 64 µg/mL, for two trials of the assay. However, the percent growth inhibition of PGG against AB5075 in regular CAMHB is close to 90% at 64 µg/mL (Figure 4.3), and so further reproductions may reveal that there is not a difference in MIC values between PGG in iron-depleted conditions and regular media. Such an interpretation may be explained by the fact that Chelex resin removes an undefined, but high amount of metal ions. Thus, the iron-depleted assay was limited because not all iron was removed from the media, allowing bacteria to utilize a small amount of iron. From these assays, I concluded that PGG interacts with iron in the environment, confirming that iron plays a role in

mediating *A. baumannii* growth and that PGG's mechanism is - at least to some extent - related to iron mediation.

Although iron is a necessary element for various metabolic processes such as cellular respiration and DNA synthesis, it is not always bioavailable for bacteria to utilize due to its low solubility in neutral and basic pH environments (Kramer, Ozkaya, & Kummerli, 2020). To document how bacteria have evolved to increase iron uptake, a large body of literature exists on bacterial siderophores, the secondary metabolites that bacteria secrete in order to sequester iron from the environment. It is likely that PGG inhibits *A. baumannii* growth by interfering with the sequestration activity of siderophores, which are encoded by clustered genes in the bacterial genome (Eijkelkamp, Hassan, Paulsen, & Brown, 2011).

To visualize the interaction of PGG with iron in the media, optical density values of PGG were obtained in iron (II) and iron (III) supplemented CAMHB. When media treated with PGG is supplemented with iron, the media becomes an opaque purple color that increases in darkness with increasing concentrations of PGG. Optical density plate readings confirmed these visual observations (Figure 4.9). The concentration-dependent color increase correlates with increased interaction of PGG and iron, which I have related to decreased inhibitory activity of PGG. To further relate the attenuated growth inhibition to iron availability in the environment, I modified the spontaneous mutant assays by adding 1 mM of iron (II) sulfate or iron (III) sulfate to AB5075 grown in media treated with different concentrations of PGG. Prior to iron supplementation, all of the PGG-treated wells (except for a single 0.5 x MIC well) exhibited no bacterial growth after 24 hours of incubation. After addition of 1 mM of iron and 24 hours of incubation, growth was restored in all of the 0.5 x MIC wells, except a single iron (III) supplemented, 0.5 x MIC well in TSA. After 48 hours of incubation following the initial addition of iron, colony density increased

in all of the wells with restored growth. Because iron supplementation and subsequent incubation were the only factors introduced, the restoration of bacterial growth can be attributed to the addition of iron. This supports the hypothesis that PGG inhibits *A. baumannii* growth by sequestering available iron in the environment.

After addition of 1 mM of iron and 24 hours of incubation, bacterial growth was also present, to a lesser degree, in the iron (II) supplemented wells of 1 x MIC in CAMHA and TSA, and two colonies were present in the iron (II) supplemented wells of 2 x MIC in TSA. Thus, bacterial density was also related to the initial concentration of PGG in the wells; the more PGG that was initially added, the less restoration of growth was seen after iron supplementation. This supports the idea that PGG interacts with iron in a concentration-dependent manner. If iron chelation is indeed PGG's mechanism of action, results suggest that the lower concentrations of PGG were only able to sequester iron already present in the media. The 1 mM iron addition - a molar addition of approximately 144:1 (iron ion: PGG) for the highest tested concentration (256 μg/mL) - overwhelmed PGG's sequestration capabilities, and thus restored bacterial chelation of necessary iron. This application of data supports Lin et al.'s conclusions that PGG is an iron chelator against *S. aureus* biofilm, for which addition of iron was shown to restore biofilm formation (Lin et al., 2012). The opposing sequestration activities of bacterial siderophores and host immune system components have been described as a "tug-of-war" for iron (Golonka, Yeoh, & Vijay-Kumar, 2019). The data and observations from this Thesis suggest that the "tug-of-war" metaphor is also apt for describing the opposing activities of *A. baumannii* siderophores and PGG. When AB5075 is treated with PGG, iron in the media interacts with PGG and is sequestered away. When iron supplementation inundates the media again, bacteria are able to chelate the necessary minerals.

In relation to published literature on PGG's biofilm inhibition activity against *S. aureus* (Lin et al., 2012), I performed biofilm formation inhibition and biofilm eradication assays on PGG against *A. baumannii* AB5075. While the former involves determining the effect of treatment on the initial creation and adherence of biofilm, the latter involves determining the effect of treatment on the elimination of already formed biofilm. Thus, the starting concentrations of treatment for the formation inhibition assay were subIC_{50} in order to quantify biofilm inhibition, rather than overall growth inhibition. For the biofilm eradication assay, this was not a concern because the goal was to quantify percentage of biofilm that could be eradicated by treatment, after biofilm was already formed. Both assays utilized tetracycline as the false positive control because although *A. baumannii* remains susceptible to this antibiotic, there is no known true positive control for biofilm inhibition of the species. The results indicate that PGG is not active against biofilm in *A. baumannii*. This differs from Lin et al.'s biofilm inhibition studies on PGG against *S. aureus* (Lin et al., 2011) (Lin et al., 2012). Lin et al. argued that PGG inhibits *S. aureus* biofilm formation, as well as aggregation and accumulation of cells during biofilm formation, and that iron supplementation can restore biofilm formation in *S. aureus*. However, the discrepancy between our results can be attributed to the differing biofilm formation and maintenance mechanisms in Gram-negative *A. baumannii* and Gram-positive *S. aureus*. A 2014 study on the effect of iron restriction on biofilm formation revealed that *A. baumannii* biofilm formation varies between strains and growth medium, without a distinct trend related to iron limitations in the medium (Gentile et al., 2014). In fact, while 66% of isolates tested in iron-limited medium had either unchanged or decreased biofilm production, 44% of isolates tested in the same conditions had increased biofilm formation. When Gentile et al. introduced deferasirox, a clinical chelator with high affinity to iron, no significant anti-biofilm activity was observed, suggesting that *A.*

baumannii is highly capable of sequestering iron in biofilm. This is in line with PGG's lack of anti-biofilm activity. From these results, it appears that PGG is capable of chelating iron from the medium to inhibit planktonic growth, but a physical or mechanistic difference in the bacteria's iron withholding capacity interferes with PGG's iron chelation capacity in biofilm.

Future directions involve growth inhibition assays of clinical iron chelators against *A. baumannii* AB5075, in order to compare the growth inhibition activity of PGG and known iron chelators. It is also possible that PGG interferes with the chelation of other metal ions that are important for *A. baumannii* growth. Another interpretation of the iron-depleted (Chelex) assay, which resulted in growth inhibition curves similar to regular CAMHB assays, is that PGG binds to other metal ions. Restoration assays may be performed by comparing the effect of supplementing media with metals such as calcium, copper, magnesium, and zinc. To chemically verify that iron is depleted from media in the presence of PGG, mass spectrometry may be performed before and after addition of PGG to media. To develop PGG as a therapeutic drug, future considerations may involve investigating the affinity of iron to PGG and bacterial siderophores; an effective iron chelator must have higher binding affinity for iron, compared to *A. baumannii* siderophores (Zhou, Ma, Kong, & Hider, 2012).

In summary, this Thesis explores the iron chelation mechanism proposed for PGG's anti-biofilm activity against *S. aureus* (Lin et al., 2011) (Lin et al., 2012), by verifying the effect of iron supplementation on PGG's growth inhibition activity against *A. baumannii*. In addition to assays showing the attenuation of PGG activity in iron-supplemented medium, spontaneous mutant assays show that PGG's inhibition activity can be overwhelmed by the addition of iron after initial PGG treatment, resulting in a restoration of bacterial growth.

Lipopolysaccharide attachment as a possible mechanism of action

Another possible target of PGG is the lipid A component of the outer membrane of Gram-negative bacteria. In a 2005 study, PGG isolated from the traditional Chinese herb, Radix Paeoniae Rubra, was found to have lipid A-binding abilities (Genfa et al., 2005). To investigate the interaction of PGG and lipids in relation to *A. baumannii*, lipid supplementation studies were performed through growth inhibition and time-kill assays of PGG against *A. baumannii* AB5075, similar to the ones performed for iron supplementation. Although 0.02% oleic acid supplementation resulted in no change in growth inhibition, 0.02% polysorbate 80 supplementation resulted in a 16-fold increase of the IC_{50} value compared to the control condition without lipid supplementation, increasing from 8 µg/mL to 128 µg/mL. Time-kill assay results also showed this discrepancy. Compared to the control condition, oleic acid supplementation resulted in an approximate 10-fold increase in CFU/mL measurements, and polysorbate 80 supplementation resulted in an approximate 100-fold increase in CFU/mL measurements. These results show that PGG's growth inhibition activity against AB5075 is attenuated by polysorbate 80 addition but is not affected to the same degree by oleic acid addition. Explanations for why PGG is more affected by one lipid over the other may include chemical and physical differences between the two tested solutions of lipids. Follow-up experiments may involve lipid supplementation assays of other commercially available lipids, as well as a comparative chemical analysis of the lipid A moiety of AB5075 and the tested lipids.

One possible explanation for the decrease in PGG's inhibition in polysorbate 80-supplemented media is that PGG's inhibition mechanism involves binding to lipids. This hypothesis agrees with Genfa et al.'s findings that PGG can bind directly to lipid A with a Kd of 32 µM, and can thus neutralize the endotoxin in vitro and decrease plasma endotoxin levels in vivo (Genfa et al., 2005). It is possible that PGG inhibits the growth of *A. baumannii* by binding to the

lipid A component of the bacteria's outer membrane. Therefore, when media was supplemented with polysorbate 80, PGG bound to the added lipid - instead of the bacteria's membrane component - and was consequently overwhelmed.

Often explored as a possible antibiotic target, the lipid A component of Gram-negative bacteria resides in the lipopolysaccharide (LPS) portion of the outer membrane (Wyckoff, Raetz, & Jackman, 1998). Previous literature regards the LPS as a significant part of Gram-negative bacteria, due to its role in interacting with host CD14 immune cells (Karima, Matsumoto, Higashi, & Matsushima, 1999). Lipid A is the toxic component of LPS, and unrestrained activation of the host immune system to this endotoxin can induce sepsis, leading to multiple organ damage and potentially, death (Wyckoff et al., 1998). Thus, a lipid A-binding chemical could prove effective against endotoxin-dispersing *A. baumannii*. In addition, the LPS forms a permeability barrier against the passive diffusion of hydrophobic molecules, such as antibiotics (Nikaido, 2003).

However, a 2010 study questioned the essentiality of LPS to all strains of Gram-negative bacteria by isolating *Neisseria meningitides*, *Moraxella catarrhalis*, and *A. baumannii* mutants without LPS (Zhang, Meredith, & Kahne, 2013). Zhang et al. found that the presence of LPS is both species and strain-dependent, and not an essential element of the outer membrane as was previously accepted. Nonetheless, LPS-null strains, such as the *A. baumannii* strains that were resistant to colistin, had higher susceptibility to non-polymyxin drugs. The LPS-null strains had decreased membrane integrity and were thus more susceptible to antibiotics. If PGG's mechanism of inhibition is indeed through binding of lipid A, these considerations may prove useful for the development of drug delivery systems. For example, a lipid A-binding drug may be utilized prior to an antibiotic, in order to disrupt bacterial membrane integrity.

Conclusion

In this study, the ethnobotanical approach to anti-infective drug discovery was validated for extracts of *S. terebinthifolia*, *R. coriaria*, and *R. copallinum*. PGG, which was previously isolated from *S. terebinthifolia*, is also a putative active compound in the ethyl acetate extracts of *R. coriaria* (extract 1271C) and *R. copallinum* (extract 1722C). The *Rhus* extracts and PGG exhibit inhibitory activity against both susceptible and resistant strains of *A. baumannii*, as well as tested *P. aeruginosa* and *S. aureus* strains. Biofilm formation inhibition and eradication assays did not show PGG to have antibiofilm activity against *A. baumannii* AB5075, which may be due to species-specific characteristics of biofilm formation and maintenance. Time-kill assays confirmed PGG to be a bacteriostatic agent against *A. baumannii*, and cytotoxicity tests yielded a therapeutic index of 32 for PGG, suggesting that the compound may be used as a topical drug.

The mechanistic studies of PGG against *A. baumannii* explored (1) chelation of iron from the environment and (2) attachment of lipids associated with the outer membrane of Gram-negative bacteria. Supplementation of media with iron (II) sulfate, iron (III) sulfate, and polysorbate 80 decreased the inhibitory activity of PGG, suggesting that PGG's mechanism(s) of action involve interaction with iron and/or lipids. However, further mechanistic studies must be performed to confirm the specific mechanism(s) of action by which PGG inhibits *A. baumannii* growth. In summation, the documented antibacterial activity of PGG, and the plants that yield this active compound, demonstrate the medical potential of traditional plants and warrant further investigation.

References

Abhau, A. (2007). *The Survival of a Malagasy Lemur Species Propithecus verreauxi coquereli in Captivity: The Vital Role of a Self-selected Plant Diet. .* Retrieved from https://d-nb.info/984680519/34

Baumann, P. (1968). Isolation of Acinetobacter from soil and water. *J Bacteriol, 96*(1), 39-42. Retrieved from https://www.ncbi.nlm.nih.gov/pubmed/4874313

Bergogne-Berezin, E., & Towner, K. J. (1996). Acinetobacter spp. as nosocomial pathogens: microbiological, clinical, and epidemiological features. *Clin Microbiol Rev, 9*(2), 148-165. Retrieved from https://www.ncbi.nlm.nih.gov/pubmed/8964033 https://cmr.asm.org/content/cmr/9/2/148.full.pdf

Botnick, I. (2012). Medieval practical medical prescriptions, found in the Cairo Genizah. In.

Bursal, E., & Koksal, E. (2010). Evaluation of reducing power and radical scavenging activities of water and ethanol extracts from sumac (Rhus coriaria L.). *Food Res Int, 44*(7), 2217-2221. doi:https://doi.org/10.1016/j.foodres.2010.11.001

Candan, F., & Sokmen, A. (2004). Effects of Rhus coriaria L (Anacardiaceae) on lipid peroxidation and free radical scavenging activity. *Phytother Res, 18*(1), 84-86. doi:10.1002/ptr.1228

CDC. (2019). *Antibiotic Resistance Threats in the United States, 2019*. Atlanta, GA: CDC

Chassagne, F., Huang, X., Lyles, J. T., & Quave, C. L. (2019). Validation of a 16th Century Traditional Chinese Medicine Use of Ginkgo biloba as a Topical Antimicrobial. *Front Microbiol, 10*, 775. doi:10.3389/fmicb.2019.00775

Cho, J. Y., Sohn, M. J., Lee, J., & Kim, W. G. (2010). Isolation and identification of pentagalloylglucose with broad-spectrum antibacterial activity from Rhus trichocarpa Miquel. *Food Chemistry, 123*(2), 501-506. doi:10.1016/j.foodchem.2010.04.072

Cockerill, F. R. (2013). *Performance standards for antimicrobial susceptibility testing: twenty-third informational supplement ; M100 - S23*. Wayne, PA: CLSI.

Comfort, J. W. (1850). Upland Sumac. In *The Practice of Medicine on Thomsonian Principles* (pp. 521-522): A. Comfort.

Cosgrove, S. E. (2006). The relationship between antimicrobial resistance and patient outcomes: mortality, length of hospital stay, and health care costs. *Clin Infect Dis, 42 Suppl 2*, S82-89. doi:10.1086/499406

Dettweiler, M., Lyles, J. T., Nelson, K., Dale, B., Reddinger, R. M., Zurawski, D. V., & Quave, C. L. (2019). American Civil War plant medicines inhibit growth, biofilm formation, and quorum sensing by multidrug-resistant bacteria. *Sci Rep, 9*(1), 7692. doi:10.1038/s41598-019-44242-y

Edwards-Jones, V. (2013). Fighting Multidrug Resistance with Herbal Extracts, Essential Oils, and Their Components. In M. R. a. K. Kon (Ed.), *Fighting Multidrug Resistance* (1 ed., pp. 1-9). San Diego, CA: Elsevier.

Eijkelkamp, B. A., Hassan, K. A., Paulsen, I. T., & Brown, M. H. (2011). Investigation of the human pathogen Acinetobacter baumannii under iron limiting conditions. *BMC Genomics, 12*, 126. doi:10.1186/1471-2164-12-126

Elias, T. S. (1987). *The complete trees of North America : field guide and natural history*. New York: Gramercy Pub. Co. : Distributed by Crown Publishers.

Facciola, S. (1990). *Cornucopia : a source book of edible plants*. Vista, CA: Kampong Publications.

Genfa, L., Jiang, Z., Hong, Z., Yimin, Z., Liangxi, W., Guo, W., . . . Lizhao, W. (2005). The screening and isolation of an effective anti-endotoxin monomer from Radix Paeoniae Rubra using affinity biosensor technology. *Int Immunopharmacol, 5*(6), 1007-1017. doi:10.1016/j.intimp.2005.01.013

Gentile, V., Frangipani, E., Bonchi, C., Minandri, F., Runci, F., & Visca, P. (2014). Iron and Acinetobacter baumannii Biofilm Formation. *Pathogens, 3*(3), 704-719. doi:10.3390/pathogens3030704

Giancarlo, S., Rosa, L. M., Nadjafi, F., & Francesco, M. (2006). Hypoglycaemic activity of two spices extracts: Rhus coriaria L. and Bunium persicum Boiss. *Nat Prod Res, 20*(9), 882-886. doi:10.1080/14786410500520186

Glenn, L. M., Lindsey, R. L., Folster, J. P., Pecic, G., Boerlin, P., Gilmour, M. W., . . . Frye, J. G. (2013). Antimicrobial resistance genes in multidrug-resistant Salmonella enterica isolated from animals, retail meats, and humans in the United States and Canada. *Microb Drug Resist, 19*(3), 175-184. doi:10.1089/mdr.2012.0177

Golonka, R., Yeoh, B. S., & Vijay-Kumar, M. (2019). The Iron Tug-of-War between Bacterial Siderophores and Innate Immunity. *J Innate Immun, 11*(3), 249-262. doi:10.1159/000494627

Howard, A., O'Donoghue, M., Feeney, A., & Sleator, R. D. (2012). Acinetobacter baumannii: an emerging opportunistic pathogen. *Virulence, 3*(3), 243-250. doi:10.4161/viru.19700

Jacobs, A. C., Thompson, M. G., Black, C. C., Kessler, J. L., Clark, L. P., McQueary, C. N., . . . Zurawski, D. V. (2014). AB5075, a Highly Virulent Isolate of Acinetobacter baumannii, as a Model Strain for the Evaluation of Pathogenesis and Antimicrobial Treatments. *MBio, 5*(3), e01076-01014. doi:10.1128/mBio.01076-14

Karima, R., Matsumoto, S., Higashi, H., & Matsushima, K. (1999). The molecular pathogenesis of endotoxic shock and organ failure. *Mol Med Today, 5*(3), 123-132. doi:10.1016/s1357-4310(98)01430-0

Kramer, J., Ozkaya, O., & Kummerli, R. (2020). Bacterial siderophores in community and host interactions. *Nat Rev Microbiol, 18*(3), 152-163. doi:10.1038/s41579-019-0284-4

Lardos, A. (2006). The botanical materia medica of the Iatrosophikon--a collection of prescriptions from a monastery in Cyprus. *J Ethnopharmacol, 104*(3), 387-406. doi:10.1016/j.jep.2005.12.035

Laxminarayan, R., Duse, A., Wattal, C., Zaidi, A. K., Wertheim, H. F., Sumpradit, N., . . . Cars, O. (2013). Antibiotic resistance-the need for global solutions. *Lancet Infect Dis, 13*(12), 1057-1098. doi:10.1016/S1473-3099(13)70318-9

Lee, C. R., Lee, J. H., Park, M., Park, K. S., Bae, I. K., Kim, Y. B., . . . Lee, S. H. (2017). Biology of Acinetobacter baumannii: Pathogenesis, Antibiotic Resistance Mechanisms, and Prospective Treatment Options. *Front Cell Infect Microbiol, 7*, 55. doi:10.3389/fcimb.2017.00055

Lev, E. (2007). Drugs held and sold by pharmacists of the Jewish community of medieval (11-14th centuries) Cairo according to lists of materia medica found at the Taylor-Schechter Genizah collection, Cambridge. *J Ethnopharmacol, 110*(2), 275-293. doi:10.1016/j.jep.2006.09.044

Lin, M. H., Chang, F. R., Hua, M. Y., Wu, Y. C., & Liu, S. T. (2011). Inhibitory effects of 1,2,3,4,6-penta-O-galloyl-beta-D-glucopyranose on biofilm formation by Staphylococcus aureus. *Antimicrob Agents Chemother, 55*(3), 1021-1027. doi:10.1128/AAC.00843-10

Lin, M. H., Shu, J. C., Huang, H. Y., & Cheng, Y. C. (2012). Involvement of iron in biofilm formation by Staphylococcus aureus. *PLoS One, 7*(3), e34388. doi:10.1371/journal.pone.0034388

Ma, H. (2011). *Isolation, structural elucidation and bioactivity evaluation of phytochemicals from New England plants: Cornus amomum Mill. (silky dogwood) and Rhus copallinum L. (winged sumac).* (Master's). The University of Rhode Island, Retrieved from https://digitalcommons.uri.edu/dissertations/AAI1491449

Ma, H., Liu, W., Navindra, S., & Dain, J. (2014). Inhibitory effects of pentagalloyl glucose from winged sumac (Rhus copallinum) on albumin glycation and the formation of advanced glycation endproducts. *The FASEB Journal, 28*(1).

Ma, H., Yuan, T., Gonzalez-Sarrias, A., Li, L., Edmonds, M. E., & Seeram, N. P. (2012). New galloyl derivative from winged sumac (Rhus copallinum) fruit. *Nat Prod Commun, 7*(1), 45-46. Retrieved from https://www.ncbi.nlm.nih.gov/pubmed/22428241

Magiorakos, A. P., Srinivasan, A., Carey, R. B., Carmeli, Y., Falagas, M. E., Giske, C. G., . . . Monnet, D. L. (2012). Multidrug-resistant, extensively drug-resistant and pandrug-resistant bacteria: an international expert proposal for interim standard definitions for acquired resistance. *Clin Microbiol Infect, 18*(3), 268-281. doi:10.1111/j.1469-0691.2011.03570.x

Marshall, B. M., & Levy, S. B. (2011). Food animals and antimicrobials: impacts on human health. *Clin Microbiol Rev, 24*(4), 718-733. doi:10.1128/CMR.00002-11

Merli, M., Lucidi, C., Di Gregorio, V., Falcone, M., Giannelli, V., Lattanzi, B., . . . Venditti, M. (2015). The Spread of Multi Drug Resistant Infections Is Leading to an Increase in the Empirical Antibiotic Treatment Failure in Cirrhosis: A Prospective Survey. *PLoS One, 10*(5). doi:ARTN e0127448

10.1371/journal.pone.0127448

Mohammadi, S., Montasser Kouhsari, S., & Monavar Feshani, A. (2010). Antidiabetic properties of the ethanolic extract of Rhus coriaria fruits in rats. *Daru, 18*(4), 270-275. Retrieved from https://www.ncbi.nlm.nih.gov/pubmed/22615627

Muhs, A., Lyles, J. T., Parlet, C. P., Nelson, K., Kavanaugh, J. S., Horswill, A. R., & Quave, C. L. (2017). Virulence Inhibitors from Brazilian Peppertree Block Quorum Sensing and Abate Dermonecrosis in Skin Infection Models. *Scientific Reports, 7*. doi:ARTN 42275

10.1038/srep42275

Nasar-Abbas, S. M., & Halkman, A. K. (2004). Antimicrobial effect of water extract of sumac (Rhus coriaria L.) on the growth of some food borne bacteria including pathogens. *Int J Food Microbiol, 97*(1), 63-69. doi:10.1016/j.ijfoodmicro.2004.04.009

Nemeth, J., Oesch, G., & Kuster, S. P. (2015). Bacteriostatic versus bactericidal antibiotics for patients with serious bacterial infections: systematic review and meta-analysis. *J Antimicrob Chemother, 70*(2), 382-395. doi:10.1093/jac/dku379

Nikaido, H. (2003). Molecular basis of bacterial outer membrane permeability revisited. *Microbiol Mol Biol Rev, 67*(4), 593-656. doi:10.1128/mmbr.67.4.593-656.2003

Nikaido, H. (2009). Multidrug resistance in bacteria. *Annu Rev Biochem, 78*, 119-146. doi:10.1146/annurev.biochem.78.082907.145923

NN, A. (2015). A Review on the Extraction Methods Use in Medicinal Plants, Principle, Strength and Limitation. *Medicinal and Aromatic Plants, 4*(3). doi:10.4172/2167-0412.1000196

Pankey, G. A., & Sabath, L. D. (2004). Clinical relevance of bacteriostatic versus bactericidal mechanisms of action in the treatment of Gram-positive bacterial infections. *Clin Infect Dis, 38*(6), 864-870. doi:10.1086/381972

Polunin, O. (1980). *Flowers of Greece and the Balkans : a field guide*. Oxford ; New York: Oxford University Press.

Price, L. B., Stegger, M., Hasman, H., Aziz, M., Larsen, J., Andersen, P. S., . . . Aarestrup, F. M. (2012). Staphylococcus aureus CC398: host adaptation and emergence of methicillin resistance in livestock. *MBio, 3*(1). doi:10.1128/mBio.00305-11

Quave, C. L., & Pieroni, A. (2015). A reservoir of ethnobotanical knowledge informs resilient food security and health strategies in the Balkans. *Nat Plants, 1*, 14021. doi:10.1038/nplants.2014.21

Richter, M. F., Drown, B. S., Riley, A. P., Garcia, A., Shirai, T., Svec, R. L., & Hergenrother, P. J. (2017). Predictive compound accumulation rules yield a broad-spectrum antibiotic. *Nature, 545*(7654), 299-304. doi:10.1038/nature22308

Said, O., Khalil, K., Fulder, S., & Azaizeh, H. (2002). Ethnopharmacological survey of medicinal herbs in Israel, the Golan Heights and the West Bank region. *J Ethnopharmacol, 83*(3), 251-265. doi:10.1016/s0378-8741(02)00253-2

Scudder, J. (1895). Transactions of the Ohio State Eclectic Medical Association.

Sebeny, P. J., Riddle, M. S., & Petersen, K. (2008). Acinetobacter baumannii skin and soft-tissue infection associated with war trauma. *Clin Infect Dis, 47*(4), 444-449. doi:10.1086/590568

Sezik, E., Yesilada, E., Honda, G., Takaishi, Y., Takeda, Y., & Tanaka, T. (2001). Traditional medicine in Turkey X. Folk medicine in Central Anatolia. *J Ethnopharmacol, 75*(2-3), 95-115. doi:10.1016/s0378-8741(00)00399-8

Shurkin, J. (2014). News Feature: Animals that self-medicate. *Proceedings of the National Academy of Sciences of the United States of America, 111*(49). doi:10.1073/pnas.1419966111

Singh, J. K., Adams, F. G., & Brown, M. H. (2018). Diversity and Function of Capsular Polysaccharide in Acinetobacter baumannii. *Front Microbiol, 9*, 3301. doi:10.3389/fmicb.2018.03301

Sturtevant, E. L. (1972). *Sturtevant's edible plants of the world*. New York,: Dover Publications.

Tipton, K. A., Dimitrova, D., & Rather, P. N. (2015). Phase-Variable Control of Multiple Phenotypes in Acinetobacter baumannii Strain AB5075. *J Bacteriol, 197*(15), 2593-2599. doi:10.1128/JB.00188-15

Torres-León, C., Ventura-Sobrevilla, J., Serna-Cock, L., Ascacio-Valdés, J. A., Contreras-Esquivel, J., & Aguilar, C. N. (2017). Pentagalloylglucose (PGG): A valuable phenolic compound with functional properties. *Journal of Functional Foods, 37*, 176-189. doi:https://doi.org/10.1016/j.jff.2017.07.045

Tripathi, P. C., Gajbhiye, S. R., & Agrawal, G. N. (2014). Clinical and antimicrobial profile of Acinetobacter spp.: An emerging nosocomial superbug. *Adv Biomed Res, 3*, 13. doi:10.4103/2277-9175.124642

Tuzlaci, E., & Aymaz, P. E. (2001). Turkish folk medicinal plants, Part IV: Gonen (Balikesir). *Fitoterapia, 72*(4), 323-343. doi:10.1016/s0367-326x(00)00277-x

USDA, N. (2020). The PLANTS Database. Retrieved from http://plants.usda.gov. from National Plant Data Team http://plants.usda.gov

van Duin, D., & Paterson, D. L. (2016). Multidrug-Resistant Bacteria in the Community: Trends and Lessons Learned. *Infect Dis Clin North Am, 30*(2), 377-390. doi:10.1016/j.idc.2016.02.004

Wald-Dickler, N., Holtom, P., & Spellberg, B. (2018). Busting the Myth of "Static vs Cidal": A Systemic Literature Review. *Clin Infect Dis, 66*(9), 1470-1474. doi:10.1093/cid/cix1127

Wang, S., Wang, H., Ren, B., Li, X., Wang, L., Zhou, H., . . . Xu, H. H. K. (2018). Drug resistance of oral bacteria to new antibacterial dental monomer dimethylaminohexadecyl methacrylate. *Sci Rep, 8*(1), 5509. doi:10.1038/s41598-018-23831-3

Wegener, H. C., Aarestrup, F. M., Jensen, L. B., Hammerum, A. M., & Bager, F. (1999). Use of antimicrobial growth promoters in food animals and Enterococcus faecium resistance to therapeutic antimicrobial drugs in Europe. *Emerg Infect Dis, 5*(3), 329-335. doi:10.3201/eid0503.990303

WHO. (2019). *2019 Antimicrobial agents in cinical development: an analysis of the antibacterial clinical development pipeline*. Retrieved from Geneva:

Wyckoff, T. J., Raetz, C. R., & Jackman, J. E. (1998). Antibacterial and anti-inflammatory agents that target endotoxin. *Trends in Microbiology, 6*(4), 154-159. doi:10.1016/s0966-842x(98)01230-x

Zhang, G., Meredith, T. C., & Kahne, D. (2013). On the essentiality of lipopolysaccharide to Gram-negative bacteria. *Curr Opin Microbiol, 16*(6), 779-785. doi:10.1016/j.mib.2013.09.007

Zhou, T., Ma, Y., Kong, X., & Hider, R. C. (2012). Design of iron chelators with therapeutic application. *Dalton Trans, 41*(21), 6371-6389. doi:10.1039/c2dt12159j